THE ROAD TO IDENTIFYING DISEASE CAUSING GENES: ASSOCIATION TESTS, GENOTYPE IMPUTATIONS, AND SAMPLING STRATEGIES FOR SEQUENCING STUDIES

by

Peng Zhang

A dissertation submitted in partial fulfillment
of the requirements for the degree of
Doctor of Philosophy
(Bioinformatics)
in the University of Michigan
2013

Doctoral Committee:

Associate Professor Sebastian Zöllner, Chair
Professor Michael L. Boehnke
Professor Margit Burmeister
Assistant Professor Jun Li
Associate Professor Noah A. Rosenberg

Dedication

To my family for their unconditional love and support!

Acknowledgments

I'm thankful to a lot of people from the Biostatistics and Bioinformatics Department for making this work possible.

First, I would like to thank my advisor Dr. Sebastian Zöllner, for introducing me to statistical genetics and population genetics, for teaching me how to think and how to do research, for giving me time and space to grow, and for being an excellent mentor to me.

I would like to thank my committee members for their help and support for my research: Dr. Noah A. Rosenberg, Dr. Mike L. Boehnke, Dr. Margit Burmeister, and Dr. Jun Li. Dr. Rosenberg has been closely involved in my second and third project. I am impressed by how knowledgeable he is in population genetics. Dr. Boehnke has also been very helpful for the advice of my graduate study and career choices. Dr. Burmeister is one of the collaborators on the first project and also been very helpful for monitoring my progress in the Bioinformatics program. Dr. Li is very helpful and quick whenever I need his help.

I am grateful to Julia Eussen from Bioinformatics for the help along my study at Bioinformatics. I would also like to thank the people at the Center for Statistical Genetics (CSG), for providing suggestions on my CSG presentations, for maintaining the clusters, for setting up conference calls and reserving conference rooms, for providing computing

support, for making my graduate life along the way easier, especially Sue Burke, Dawn Keene, Peggy White, Laura Scott, Hyun Ming Kang, William Wen, Tom Blackwell, Sean Caron and Terry Gliedt.

I would like to thank my friends in Bioinformatics and Biostatistics, especially Yun Li, Liming Liang, Wei Chen, Jun Ding, Xiaowei Zhan, Youna Hu, Bingshan Li, Meihua Wu, Xuejing Wang, Ryan Welsh, Adrian Tan, Mark Reppell and people from Dr. Zöllner’s lab, especially Matt Zawistowski, Shyam Gopalakrishnan, Yancy Lo, and Ziqian Geng.

I want to thank my family for their support along my long journey of graduate study.

Table of Contents

List of Figures

List of Tables

List of Abbreviations

BP: Bipolar disorder

GWAS: Genome-wide association studies

MAF: Minor allele frequency

SNP: Single nucleotide polymorphism

Abstract

THE ROAD TO IDENTIFYING DISEASE CAUSING GENES: ASSOCIATION TEST, GENOTYPE IMPUTATIONS, AND SAMPLING STRATEGIES FOR SEQUENCING STUDIES

by

Peng Zhang

Chair: Sebastian Zöllner

Technological advances now allow investigators to use sequencing data to identify genetic risk variants for complex diseases. However, it is still expensive to sequence a large sample of individuals. While genotype imputation can augment sequence studies, challenges still remain, such as imputation with population or family structures and imputation of rare variants. This dissertation aims to tackle these two challenges.

The first project considers imputation with family structures, which extended from an existing imputation program that assumes unrelated individuals in a sample. I propose a strategy for imputing data with family structures and apply it to a family-based association study for bipolar disorder. The results suggest the involvement of ion channelopathy in bipolar pathogenesis.

The second and third projects provide sampling strategies for next-generation sequencing. The goal is to select a subset from a study sample that incorporates maximal number of variants when sequenced, or to achieve maximal imputation accuracy when impute the sequences of the rest study sample using the sequenced subset or both. In the second project, I propose the "most diverse panel" by adapting the concept of the phylogenetic diversity. This strategy assumes that the panel with the biggest overall tree length in the phylogenetic tree represents the longest evolutionary time, allowing the maximal number of mutation events to occur. Sequencing such a panel can thus identify the maximal number of variants. In the third project I propose the "most representative panel" by considering both the selected and unselected haplotypes. The goal is to identify at least one optimal selected reference haplotype for each unselected haplotype. Because it is computationally impossible to perform an exhaustive search for a large sample size, I develop a hill-climbing algorithm that updates a randomly selected panel a predefined number of iterations or until it converges. Using simulated sequence data and real sequence data from the 1000 Genomes Project, I compare the two proposed panels to randomly selected panels and provide suggestions on which algorithm to use when planning sequencing studies with specific study samples.

Chapter 1 Introduction

On the road to identifying disease-causing genes, investigators have successfully identified many common variants that are associated with complex diseases through GWAS since 2005 (http://www.genome.gov/gwastudies/). However, the fact that those identified common variants can only account for a very small proportion of disease inheritability motivates investigators to study rare variants for complex diseases. With the dramatic cost reduction in next-generation sequencing, investigators start to sequence previous samples from GWAS, either by candidate regions or the whole genomes, to identify rare risk variants that contribute to the missing disease inheritability. However, sequencing a large sample is still expensive. Genotype imputation can augment sequence data. In this dissertation, I address how to perform genotype imputation with structured data and how we can use genotype imputation in sequencing studies.

Genotype imputation is an important tool in disease gene mapping and has been widely used in association studies. It typically uses a densely genotyped panel to predict the genotypes in a less densely genotyped study sample (Li et al. 2009). Genotype imputation allows direct testing of untyped markers for associations with phenotypes of interest and can increase the power for identifying genetic risk variants for complex diseases (Li et al. 2009; Marchini and Howie 2010). Genotype imputation is often used in meta-analysis to combine samples that are genotyped on different platforms (Zeggini et al. 2008; Scott et al. 2009). Currently the most often used genotype imputation programs include MaCH

(Li et al. 2010), *minimac* (Howie et al. 2012), IMPUTE (Marchini et al. 2007), IMPUTE2 (Howie et al. 2009), and BEAGLE (Browning and Yu 2009). All these programs are implemented based on a hidden Markov model, modeling samples as unrelated individuals. While each imputation program may provide different imputation quality for a specific study sample, reference panel selection affects more in imputation accuracy in genotype imputation. Previous studies showed that imputation accuracy was higher when the reference panel and the study sample derive from the same or similar populations than when they are from substantially different populations (Huang et al. 2009).

In Chapter 2, I conduct a family-based association study for identifying genetic risk variants for bipolar disorder in the chromosome 8q24 region. This is a follow-up study to narrow down the genetic risk variants that could explain a previously observed linkage peak at 8q24 (McInnis et al. 2003; McQueen et al. 2005). McInnis et al. (2003) performed a genome-wide scan for bipolar disorder in 65 pedigrees and showed the top linkage signal at 8q24 for suggestive evidence of linkage. McQueen et al. (2005) performed a meta-analysis that combined 11 studies, including the study by McInnis et al. (2003), and reported a genome-wide significant LOD score of 3.4 at 8q24. Using family data including the families used in the previous linkage analysis, my collaborators genotyped over 3000 SNPs across the 123.1 to 139.1 Mb region at 8q24 for 3,512 individuals from 737 families (Zandi et al. 2007; Zandi et al. 2008; Zhang et al. 2010). I perform a detailed family-based association analysis to evaluate the correlations between the common genetic variants in this region to bipolar disorder. In addition, I propose a novel strategy for imputing genotypes with family-based data and perform genotype imputation to get the genotypes of all the international HapMap markers for our data (The International HapMap Consortium 2005). To extend the imputation of related individuals, I perform the imputation in two steps by first calibrating imputation parameters using a subset of the study sample with unrelated individual, and then conduct the imputation on the entire study sample. In addition, I show that family structure can additionally filter out poor imputed markers not detected by other quality control measures. The results show suggestive evidence of association between bipolar disorder and loci near three genes. Consistent with genes identified by genome-wide association studies for bipolar disorder (Ferreira et al. 2008), the results indicate the involvement of ion channelopathy in bipolar pathogenesis.

Investigators have performed many genome-wide association studies (GWAS) to test for associations of common variants with complex diseases, and have identified thousands of SNPs associated with diseases of interest Since 2005 (http://www.genome.gov). However, many of these findings in one study are not replicated in other GWAS, possibly due to their population differences or the heterogeneity of diseases. The search for genetic variants in psychiatric disorders is especially difficult because of their extreme heterogeneity in clinical features, diagnosis, and interactions with environmental factors (Van Os et al. 2008; Scott et al. 2009; Zhang et al. 2010). So far, only a few large meta-analyses of schizophrenia and bipolar disorder reported genome-wide significant associations, as reviewed recently by Lee et al. (2012).

The design of GWAS is to target the common variants (e.g., minor allele frequency > 0.05) in the genome. Although many GWAS have successfully identified common risk variants that are significantly associated with traits of interests, those genetic variants combined only contribute to a very small proportion of the observed genetic component (Bodmer and Bonilla 2008). On the other hand, less common risk variants, such as variants with minor allele frequency less than 0.05, often have large effect sizes for disease risk (Cohen et al. 2004; Gibson 2011). With dramatic cost reduction in next-generation sequencing technology, investigators were able to identify rare genetic risk variants through sequencing studies (Shendure and Ji 2008; Li et al. 2011). In principle, sequencing can identify most variants in a study sample, especially novel rare variants (Cirulli and Goldstein 2010). One caveat, however, is that the rarer of variants, the bigger sample sizes are needed to achieve the statistical power for the association testing. Sequencing study samples at the GWAS scale is still prohibitively expensive in many studies. Thus sampling strategies are often needed for selecting an optimal subset of the study sample to sequence. The sequenced subset can then be used as a reference panel to impute the rest of the study samples.

In Chapter 3, I introduce an idea of phylogenetic diversity from mathematical phylogenetics and comparative genomics and propose the “most diverse reference panel”, defined as the subset with maximal “phylogenetic diversity”. The identification of subset with maximal diversity has been a common practice in other area of genetics, such as biodiversity conservation (Faith 1992; Steel 2005) and biodiversity genome sequencing (Pardi and Goldman 2005). The strategy assumes that the panel with the biggest overall tree length in the phylogenetic tree represents the longest evolutionary time, which allows the maximal number of mutation events to occur. Sequencing such a panel can thus identify the maximal number of variants.

In Chapter 4, I present another sampling strategy for planning sequencing studies. Instead of focusing on maximizing phylogenetic diversity in the selected subset, I aim to maximize the similarity between haplotypes in the selected subset (R) and haplotypes in the unselected subset (U) by minimizing a distance metric I defined between R and U. To locate this optimal realization, an exhaustive search is not computationally feasible for a large sample size due to the combinatorial nature of this problem, and there are no existing alternative algorithms available. Here I adapt a local search algorithm, the hill-climbing search, to find a local optimum of R and U. To speed up the search and to avoid the algorithm being stuck in a local optimum, I randomly start multiple times and choose the one with minimum (R, U) distance as the starting status for the hill-climbing update. The goal is to get the global optimum or a local optimum distance that is a reasonable approximation of the global optimum (Selman and Gomes 2006).

Using simulated sequence data and real sequence data from the 1000 Genomes Project, I compare the two proposed panels to randomly selected panels. The results show that both the most diverse panel and the representative panel incorporate more sites that are polymorphic and also provide better imputation accuracy when used as reference panels than randomly selected panels. The major advantage here is the genotypes for extra variants gained by the propose panel without experimental cost than using a randomly selected panel. I also compare the performance of the two proposed strategies under different settings, such as reference size, imputation length, and maker density in the study sample. In the end, I provide some suggestions on which algorithm to use when planning sequencing studies with specific study samples based on the observed results and outline future directions I plan to extend the current work.

Chapter 2 A family-based association analysis to finemap linkage peak on 8q24 for bipolar disorder

2.1 Introduction

Bipolar disorder (BP) is a common, complex psychiatric disease characterized by recurrent depression and manias, with an estimated lifetime prevalence of ~1% (Merikangas et al. 2007). Family and twin studies have reported a strong familial aggregation of BP, suggesting that genetic factors account for 60% to 85% of disease risk (Smoller and Finn 2003). While a large number of genetic variants were reported to be either linked or associated with BP, few have been replicated (Burmeister et al. 2008; Serretti and Mandelli 2008). Only recent large genome wide association studies (GWAS) were able to identify the first BP genes. Ferreira et al. (Ferreira et al. 2008) analyzed a combined sample of 4,387 BP patients and 6,209 controls and reported genome-wide significant associations to BP with SNPs in Ankyrin 3 (*ANK3*) and in the alpha 1C subunit of the L-type voltage-gated calcium channel (*CACNA1C*), and the same SNPs in both *ANK3* (Scott et al. 2009) and *CACNA1C* (Ferreira et al. 2008) were replicated by independent studies. However, these two variants account only for a small proportion of BP's heritability, most heritable risk remains unexplained.

Some of this heritability may be explained by variants located in regions previously identified by linkage studies. Since the development and subsequent evolution of the human genome map and modern mapping methodologies, over 40 genome-wide linkage reports on BP and at least three meta-analysis (Badner and Gershon 2002; McQueen et al. 2005) were published [for review see (Barnett and Smoller 2009)]. We first reported linkage to BP on 8q24 region with an NPL score of 3.25 (Dick et al. 2003; Avramopoulos et al. 2004). Cichon et al. (2001) also reported a genome-wide significant two-point LOD score (*D8S514*; LOD = 3.62) at 8q24 in a genome-wide linkage scan of 75 BP families (Cichon et al. 2001). These results were included in a meta-analysis of 11 studies by McQueen et al. (2005), which reported a genome-wide significant LOD score of 3.40 in a region on chromosome 8q24 under a broad model of BP (BPI and BPII) (McQueen et al. 2005). Moreover, Macayran et al. (2006) reported a child with BP carrying a duplication of 8q22.1- q24.1 caused by an unbalanced translocation (Macayran et al. 2006).

To identify genetic variants that account for the linkage signal in this region, we have previously performed an association analysis with 249 candidate gene SNPs covering a 3.4 Mb region in a sample of 583 affected offspring from 258 nuclear families with evidence of linkage to BP. We detected suggestive level of associations with SNPs three kb upstream of *ST3GAL1* (Zandi et al. 2007). We further typed an extended sample of 3,512 individuals from 737 multiplex families for 1,458 SNPs across a ~16 Mb region on 8q24. We tested each marker for association with BP, and found suggestive, but not experiment-wide significant associations with SNPs in several genes (Zandi et al. 2008).

However, this SNP panel tagged (r^2 > 0.8) only ~ 54% of known common polymorphisms in the 8q24 region (Zandi et al. 2008). To fill the gaps we designed a complementary panel of 1,536 additional SNPs in the same 8q24 region and typed the panel on the same sample (Zandi et al. 2008). Here we present the joint analysis of all 3,072 SNPs. Furthermore, we developed an approach to apply the imputation method MACH to family-based data. We imputed 22,725 HapMap SNPs in a ~ 18 Mb regions on 8q24 flanking the linkage peak reported by McQueen et al. (McQueen et al. 2005). We tested all variants for association to bipolar disorder under several genetic models, and obtained evidence of suggestive level of association between BP with loci near *KCNQ3*, *ADCY8*, and *ST3GAL1*. None of the observed associations are sufficient to account for the previous reported linkage signal.

2.2 Materials and Methods

2.2.1 Samples

The study combined the Johns Hopkins sample of 65 families and the NIMH sample of 672 families; both samples have been described elsewhere [for Hopkins sample (Dick et al. 2003); and for NIMH sample (Dick et al. 2003) (Dick et al 2003, McInnis et al. 2003, NIHM Human Genetics Initiative Web Site)]. Both samples collected multiplex families segregating BP, ascertained for a linkage study of BP. Family members were assessed using the Schedule for Affective Disorders - Lifetime Version (SADS-L) (Endicott and Spitzer 1978) or the Diagnostic Interview for Genetic Studies (DIGS) (Nurnberger et al. 1994). Diagnoses of BPI and SABP were based on Research Diagnostic Criteria (RDC) in the first sample and DSM-III-R in the second sample (criteria are essentially the same). BPII diagnosis was based on RDC with the additional requirement of recurrent major depression. The final best estimate diagnosis procedure engaged two non-interviewing psychiatrists to review all the data for a consensus clinical diagnosis. In the case of disagreement a third psychiatrist reviewed discordant diagnoses and adjudicated a final diagnosis.

Our sample comprised 3,525 genotyped individuals including 1,383 males and 2,129 females from 737 families (Zandi et al. 2008). As the initial linkage peak was obtained using a broad definition of affection status, we defined individuals diagnosed with BPI, schizo-affective disorder, SABP or BPII as affected (n = 1,958), and individuals who were determined to be never mentally ill as unaffected (n = 515). The remaining individuals were defined as missing disease status (n = 1,052).

2.2.2 Genotype data

Genotype data was collected in two phases. We selected 1,536 SNPs in the region from 123.1 to 139.1 Mb (Build 35) on chromosome 8q24 using FESTA (Gopalakrishnan and Qin 2006) for the first phase that was performed at the Center of Inherited Disease Research (CIDR) (Zandi et al. 2008). We aimed to tag all the known common variants (minor allele frequency, MAF > 0.05) with $r^2 \geq 0.5$ in region 123 to 131 Mb and $r^2 \geq 0.8$ in region 131 to 139 Mb. 1,461 SNPs passed quality control and were included in the final analysis.

To improve coverage, we selected and typed additional 1,536 SNPs conditional on the first marker set using FESTA (Gopalakrishnan and Qin 2006) We designed this marker set to maximize the number of SNPs tagged using the same r^2 criteria as in phase I.

Moreover, we retyped 24 SNPs from phase I to estimate genotyping error rates. All markers were selected to have an Illumina design cut-off score of 0.6, per manufacturer's instruction, to generate a customized Illumina panel of 1,536 SNPs. These SNPs were genotyped using the University of Michigan's Department of Psychiatry/MBNI microarray core facility on a local Illumina Bead Station system, following manufacturer's instruction.

Quality control of the phase II data used PEDSTATS (Wigginton and Abecasis 2005). We removed all SNPs that did not satisfy all of the following criteria: successful genotyping rate ≥ 90%; number of Non-Mendelian Inheritance (NMI) errors < 6; Hardy-Weinberg equilibrium (HWE) test using the entire sample with p value $\geq 10^{-6}$; and MAF ≥ 5%. After applying these quality control criteria, we retained 1,295 SNPs of the 1,536 for analysis for a combined dataset of 2,756 SNPs.

2.2.3 Statistical Analysis

2.2.3.1 Single marker association analysis

We performed single marker association tests with program LAMP (Gargus 2006), a maximum likelihood method that jointly models linkage and association, to incorporate the large family sizes in our dataset (maximum family size, 23). For our main analysis, we assumed a multiplicative model with a population prevalence of 1%. In addition, we compared to the results obtained under dominant/recessive and a free model without any genetic model assumptions.

2.2.3.2 Imputation

We used the program MACH to impute genotypes for all markers in this 8q24 region using the CEU population from HapMap (Build 35) database as references (Macayran et al. 2006). MACH implements a hidden Markov model to impute unknown SNP genotypes, modeling samples as unrelated individuals. To extend the algorithm to related individuals, we performed MACH in two steps by first selecting 200 independent individuals to calibrate imputation parameters such as the estimates of imputation error rates. Based on these estimates we then imputed genotypes for the entire sample treating individuals as independent. In total, we imputed 22,725 SNPs in an 18 Mb region by expanding one Mb at each end of our genotyped region.

We evaluated imputation quality using three statistics. First, we estimated imputation error rates by masking 2% of the original genotypes before imputation and then comparing the true genotypes with their imputed counterparts. Second, we assessed the distribution of the quality measure $\hat{r}^2$ calculated by MACH, which is an estimate of the squared correlation between imputed genotypes and true genotypes. We excluded markers with $\hat{r}^2 < 0.3$ (n = 4,225), which has been shown to remove ~70% of badly imputed SNPs (Barnett and Smoller 2009). Moreover, the family structure in our dataset allowed us to estimate the imputation quality by counting the number of NMIs for each imputed SNPs. We removed imputed SNPs that had > 30 NMIs (n = 1,042). We also excluded SNPs that had MAF < 5% (n = 1,905). A total of 15,552 SNPs were included in the final association analysis.

2.3 Results

2.3.1 Genotype quality and coverage

We estimated the genotyping error rate by comparing genotypes of 24 SNPs that were typed in both phases for all individuals. The estimated average mismatch rate was 0.26% per SNP. Both marker sets together covered 94.1% of the common HapMap SNPs (MAF > 0.05) in the 8q24 region, they were either genotyped or covered at $r^2 \geq 0.50$, while 78.3% of those were either genotyped or covered at $r^2 \geq 0.80$.

2.3.2 Single marker association analysis

We carried out the association tests of each SNP with BP under various genetic models using LAMP. Here we reported results from a multiplicative model with a disease prevalence of 1%. The most significantly associated marker was rs2673582 ($p = 4.80\times10^{-5}$), which located 27 Kb upstream of *KCNQ3* (**Figure 2.1**). Three other SNPs had p-values $< 10^{-3}$, including rs4871780 ($p = 1.20\times10^{-4}$), rs3750889 ($p = 5.0\times10^{-4}$) and rs1023096 ($p = 7.0\times10^{-4}$). Both rs3750889 and rs1023096 are located within *ADCY8* gene and are in high linkage disequilibrium ($r^2 = 0.86$) (**Table 2.1**). Result obtained under a dominant/recessive model or a free model was not fundamentally different from these results (data not shown).

2.3.3 Imputation

To assess the performance of the imputation method MACH on family-based data, we randomly masked 2% of genotypes and treated them as missing, then estimated the performance by comparing the imputed genotypes to the true genotypes. The estimated imputation error rate was 0.0577 per genotype and 0.035 per allele, respectively. We further assessed the quality of imputed genotypes for each marker using both the number of NMIs among imputed SNPs and the estimated $\hat{r}^2$ values generated by MACH. 4,225 markers failed only the $\hat{r}^2$ -criteria, 1,145 failed only the NMI-criteria and 103 markers failed both. While the numbers of NMIs and the imputation $\hat{r}^2$ were negatively correlated (coefficient, -0.41), removing imputed SNPs by the number of observed NMIs provided an additional filter for identifying poorly imputed markers.

We tested the imputed genotypes of 15,552 SNPs for association with BP using LAMP. Our results showed 11 SNPS with p-values $<10^{-4}$ level, with the most significant being rs4339604 ($p = 9.4\times10^{-6}$, MAF = 0.057, physical position = 128.93 Mb), followed by rs7824868 ($p = 2.1\times10^{-5}$, MAF = 0.11, physical position = 128.59 Mb) (**Figure 2.2**). Note that the most significant result near 128 Mb is located in a gene desert.

2.4 Discussion

We analyzed a sample of 3,512 individuals in 737 families and tested 2,756 genotyped SNPs spanning ~16 Mb across the previously identified linkage peak in 8q24 region (McQueen et al. 2005). Furthermore, we imputed and tested all common HapMap SNPs in this region. Among the genotyped markers, the most significantly associated SNPs are located close to 133 Mb near *KCNQ3*, which is consistent with the linkage peak identified by genome-wide linkage analysis. Our result provided further suggestive evidence that supported genetic variants in *ST3GAL1* or *ADCY8* may be associated with BP (**Table 2.1**) (Zandi et al. 2007; Zandi et al. 2008). This association signal is more significant than our previous results (Zandi et al. 2008), it is difficult to assess experiment-wide statistical significance. Correcting for the number of sequenced markers tested results in a corrected p = 0.13, for the most significant finding (4.8 x 10^{-5}). However, Bonferroni correction assumes independent tests and the SNPs in this region are highly correlated. Moreover, permutation analysis cannot be applied to assess significance because of the family structure in our dataset. Hence it is not clear how to assign experiment-wide significance levels. Including imputed SNPs added additional signals with suggestive evidence for association, although no SNPs were significant after stringent (Bonferroni) correction for multiple testing.

All genes implicated by our analysis have previously been implicated as candidates for bipolar and other psychiatric disorders. *KCNQ3* has been shown to be expressed highly specific to brain and co-expressed with *KCNQ2* in most brain regions (Schroeder et al. 1998). *KCNQ2* has been implicated to be associated with BP through phosphatidyl-inositol phosphate pathway (Carter 2007) and both *KCNQ2* and *KCNQ3* are key components to form a voltage-gated potassium channel that is important in the regulation of neuronal excitability (Schroeder et al. 1998). Although no peer-reviewed evidence has been forthcoming on *KCNQ3* as a susceptibility gene for BP disorder, a recent published US patent proposed using a single nucleotide mutation in *KCNQ3* gene to assess the presence of or predisposition to schizophrenia, BP or a related mental disorder in a subject (Chumakov et al. 2006). Furthermore our findings have an intriguing connection to replicated GWAS results. *ANK3* anchors voltage-gated sodium channels, and both *ANK3* and subunits of the calcium channel are down-regulated in response to lithium treatment in mice (McQuillin et al. 2007). Hence, both the results from *ANK3* and that of *KCNQ3* support the involvement of an ion channelopathy in bipolar disorder (Gargus

2006), which was also supported by pathway-based analyses on GWAS data in BP (Askland K et al. 2009).

The product of *ADCY8* catalyzes the formation of cyclic AMP from ATP, where cyclic AMP may be involved in BP pathogenesis as a target for lithium and other mood stabilizing agents (Perez et al. 2000; Stewart et al. 2001). Malsen et al. showed that *ADCY8* was differentially expressed in specific brain region as a function of avoidance behavior in mice. The author further explored the human homologous 8q24 region using a candidate gene approach to test association with BP with genotypes from a GWAS and reported nominally significant associations with *ADCY8* (p = 0.0055) and *KCNQ3* (p = 0.0029) (De Mooij-van Malsen et al. 2009).The product of *ST3GAL1* gene is a type II membrane protein that catalyzes the transfer of sialic acid from CMP-sialic acid to galactose-containing substrates. A recent family-based association of candidate genes reported evidence of association of *ST3GAL1* to BP (empirical p value < 0.005) (Ferreira et al. 2008).

As none of the signals we observed can sufficiently explain the linkage signal in 8q24, it is likely that additional BP-variants exist in this region. However, as testing 15,552 additional imputed SNPs did not generate additional interesting signals, our panel of 2,756 SNPs likely captured most of the common haplotype variation in the 8q24 region. Therefore, typing additional common variants in this region would not result in new findings. Our results clearly show that the common variants in the 8q24 region do not explain the previously observed linkage peak (Dick et al. 2003). This result may be explained by one of two reasons: (1) The linkage peak may be a false positive, and the replications of the linkage peak are the result of publication bias. (2) The causal genetic variants in this region may be individually rare SNPs or copy number variants, which association tests of common SNP markers have low power to detect. To assess the contribution of rare variants in 8q24, it will be necessary to sequence a set of candidate genes, or the entire 8q24 region in a sample of BP cases. Our results pinpoint to at least two potential starting points.

In summary, we identified three biologically feasible signals for association with BP but more research is required to understand the contribution of genes in the 8q24 region to bipolar disorder.

Table 2.1 Top 10 results of single marker association tests. Results are for genotyped markers. I performed the tests under a multiplicative model with a disease prevalence of 1% using LAMP (Gargus 2006).

Marker	Position(Mb)	MAF	Gene	Location	LOD	P value
rs2673582	133.59	0.425	KCNQ3	27Kb upstream	3.59	4.80E-05
rs4871780	128.36	0.421			3.20	1.20E-04
rs3750889	132.07	0.406	ADCY8	intron	2.63	5.00E-04
rs1023096	132.10	0.419	ADCY8	intron	2.49	7.00E-04
rs6986303	134.55	0.289	ST3GAL1	intron	2.32	1.10E-03
rs6984550	133.63	0.200	KCNQ3	64Kb upstream	2.27	1.20E-03
rs10095649	135.23	0.133			1.96	0.0026
rs4523235	132.31	0.303			1.95	0.0027
rs10094837	135.27	0.138			1.93	0.0028
rs17602731	133.59	0.314	KCNQ3	32Kb upstream	1.89	0.0032

MAF: minor allele frequency

Figure 2.1 LocusZoom plot of association results for genotyped markers. The top figure shows p values (-$log_{10}p$) from association test for each genotyped SNPs versus position (Mb) across linkage peak on 8q24 (McQueen et al. 2005). The bottom figure magnifies one Mb surrounding the most significant maker rs2673582 (purple diamond). Below each plot, a subset of genes in this region is shown. Light gray lines display recombination rates as estimated from the HapMap data. The colors of the circles indicate the strength of linkage disequilibrium (LD) with rs2673582.

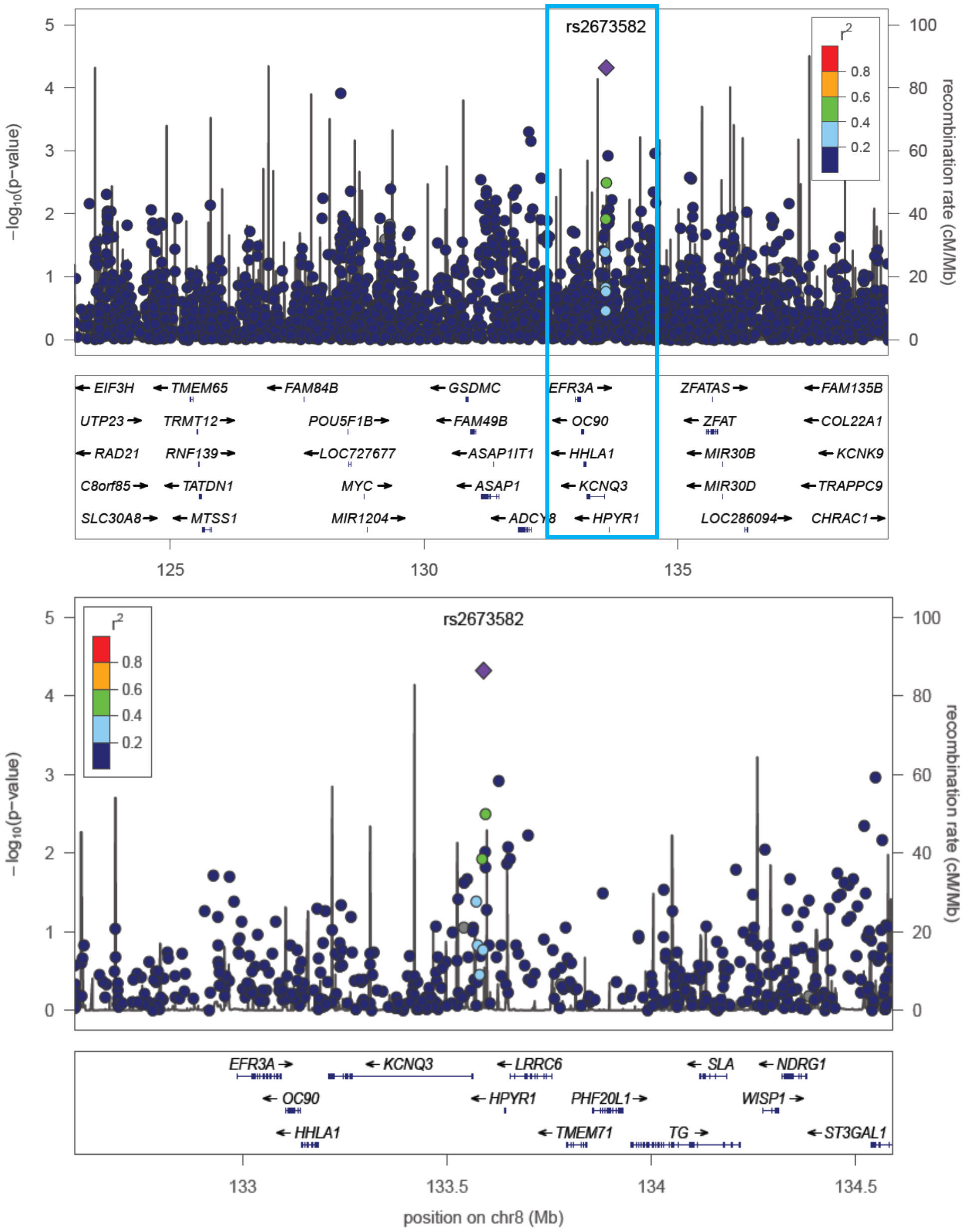
rs2673582
−log10(p−value)
recombination rate (cM/Mb)
r2
0.8
0.6
0.4
0.2
EIF3H
TMEM65
FAM84B
GSDMC
EFR3A
ZFATAS
FAM135B
UTP23
TRMT12
POU5F1B
FAM49B
OC90
ZFAT
COL22A1
RAD21
RNF139
LOC727677
ASAP1IT1
HHLA1
MIR30B
KCNK9
C8orf85
TATDN1
MYC
ASAP1
KCNQ3
MIR30D
TRAPPC9
SLC30A8
MTSS1
MIR1204
ADCY8
HPYR1
LOC286094
CHRAC1
125
130
135
rs2673582
EFR3A
KCNQ3
LRRC6
SLA
NDRG1
OC90
HPYR1
PHF20L1
WISP1
HHLA1
TMEM71
TG
ST3GAL1
133
133.5
134
134.5
position on chr8 (Mb)

Figure 2.2 LocusZoom plot of association results for all markers. P values (-$log_{10}p$) for association of genotyped and imputed SNPs on 8q24. The horizontal axis shows position in Mb. The purple diamond indicates the most significant SNP rs4339604. A subset of genes in this region is shown below the main plot. The gray lines indicate recombination rates as estimated from the HapMap data.

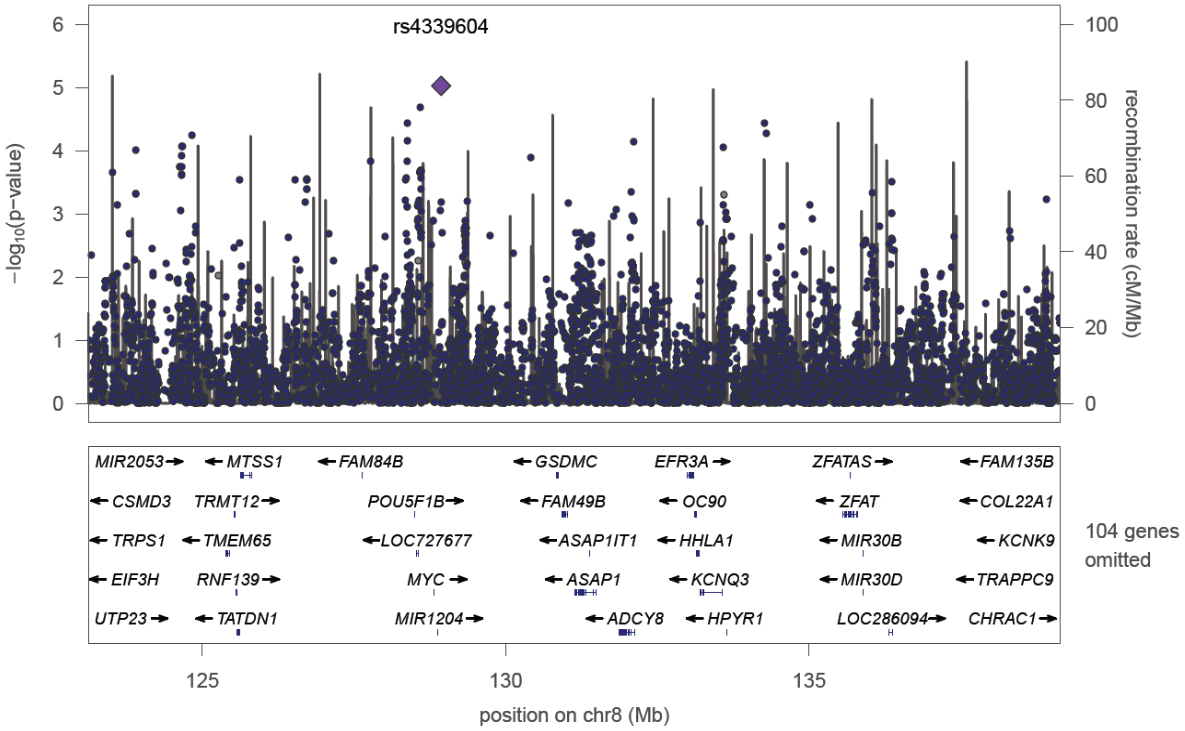

Chapter 3 Genotype imputation reference panel selection using maximal phylogenetic diversity

3.1 Introduction

Genotype imputation is an essential component of modern genetic association studies. This technique enables direct testing of untyped markers for associations with phenotypes of interest, thereby increasing the power to identify causal variants in association studies (Li et al. 2009). Imputation is especially useful in meta-analyses that combine data from genome-wide association studies (GWAS) performed using different genotyping platforms (Zeggini et al. 2008; Scott et al. 2009). Moreover, genotype imputation performed using study-specific sequenced samples enables analysis of rare variants in large GWAS genotyped datasets (Zawistowski et al. 2010).

Imputation methods typically use a reference panel of densely genotyped haplotypes to predict the missing genotypes in a less densely genotyped study sample. The choice of the reference panel then influences the imputation accuracy obtained in the study sample. It has been observed that in general, imputation accuracy is higher when the reference panel and the study sample derive from the same or similar populations than when they are from substantially different groups (Huang et al. 2009; Huang et al. 2011). However, high-diversity reference panels also contribute to increased imputation accuracy. Huang et al. (2009) found that increasing reference panel diversity by incorporating a mixture of different HapMap populations could increase imputation accuracy in comparison with the use of only a single HapMap population. Similarly, in imputing a study sample from a British birth cohort, Jostins et al. (2011) found that adding to the reference panel a proportion of HapMap samples from other populations (e.g., taking 17% of the reference panel from Toscani or 22% from Chinese and Japanese) yielded a higher imputation accuracy than using Northern European samples alone.

Most studies performed to date have selected reference panels from external databases such as the International HapMap Project (The International HapMap Consortium 2005; Frazer et al. 2007) and the 1000 Genomes Project (The 1000 Genomes Project Consortium 2010). Dramatic reductions in sequencing cost now enable an alternative strategy: to select an *internal* reference panel for genotype imputation, that is, to sequence a subset of the study sample itself and then to use the sequenced subset as a reference panel for imputing the rest of the study sample. Using reference sequences derived from the study sample can prevent a mismatch in ancestral background between the study population and the reference population. It also enables novel variants distinctive to the study sample to be imputed. Employing sequences from a candidate gene and the 1000 Genomes Project, Fridley et al. (2010) demonstrated the feasibility of imputing genetic variants based on a sequenced proportion of a study sample, and they suggested sequencing “the largest and most diverse” subset. In a theoretical study, Jewett et al. (2012) found that including sequenced haplotypes from the study population in the reference panel improved imputation accuracy, even if the external panel was taken from a closely related population. Here, we develop criteria for the selection of an internal reference panel for genotype imputation. Our goal is to find a sensible approach for choosing an internal reference panel from the study sample, with the aim of 1) maximizing the number of polymorphic sites in the imputed dataset and 2) achieving the maximal imputation accuracy.

The identification of maximally diverse subsets of a larger set of individuals has been a goal in other areas of genetics, such as in choosing diverse sets of plant accessions for inclusion in core collections targeted for agronomic development or experimental use (Brown 1989; McKhann et al. 2004; Reeves et al. 2012) and in choosing diverse species sets for biodiversity conservation (Faith 1992; Steel 2005) and genome sequencing (Pardi and Goldman 2005). In selecting a set of imputation templates, we borrow the concept of "phylogenetic diversity" which, for a given subset of a larger set of taxa, measures the fraction of the total branch length of an evolutionary tree of the larger set that is included in the restriction of the tree to the taxon subset (Faith 1992; Nee and May 1997; Steel 2005). Conditional on a tree of n taxa, Pardi and Goldman (2005) and Steel (2005) proved that among all possible subsets of size $m \leq n$ taxa from the larger set, the globally maximal phylogenetic diversity can be obtained by a greedy algorithm. This greedy algorithm provides a computationally efficient solution to a form of combinatorial optimization problem that can usually only be solved via exhaustive analysis of all possible subsets. Further, if it becomes possible for investigators to increase the number of sequenced samples, for example, by an increase in budget, then the greedy algorithm guarantees that all of the previously selected individuals will be included in the larger optimal subset.

We propose the use of the most diverse reference panel for genotype imputation, adapting the greedy algorithm for maximizing phylogenetic diversity in our selection of an internal reference panel. We assume phased diploid individual genotypes are available, as phasing is not our focus. We approximate the ancestral relationships of haplotypes by constructing a neighbor-joining phylogenetic tree (Saitou and Nei 1987) using the pairwise Hamming distance matrix between the haplotypes in a study sample (**Figure 3.1**). We next apply the greedy algorithm of Pardi and Goldman (2005) and Steel (2005) to identify the subset at a given size with the maximal "phylogenetic diversity" conditional on the tree. Similar to a method of template selection by Pasaniuc et al. (2010), our approach is tree-based, but we aim to choose a maximally diverse subset, whereas Pasaniuc et al. (2010) select a subset from an external dataset based on similarity between haplotypes in the external dataset and each individual haplotype in the study sample. The haplotypes chosen by our method are spread across the tree and tend to have long external branch lengths (**Figure 3.1**, bold lines), as our method prioritizes individual sequences that are more differentiated. We expect that in comparison with a random subset, the subset that is most phylogenetically diverse at the genotyped markers also carries a larger number of polymorphic sites that can be identified by sequencing, and that are then available for imputation into the remaining sample when this sequenced subset is used as a reference panel. Thus, this strategy enables more variants to be imputed in the study sample than with the use of a randomly selected reference panel.

Kang and Marjoram (2012) recently proposed a similar tree-based sample-selection strategy for next-generation sequencing. Their method selects a subset based on the unweighted pair group method with arithmetic mean (UPGMA) (Sokal and Michener 1958), which is designed for ultrametric data in which each haplotype has the same distance to the root of the constructed tree. The subtree identified by the method of Kang and Marjoram (2012) also requires the ultrametric assumption in order to have a maximal tree length. In contrast, the neighbor-joining method we use does not require data to be ultrametric.

To evaluate the performance of our "most diverse reference" panel in genotype imputation, we simulate sequences and create study samples similar to those observed in GWAS by masking the genotypes for a number of single nucleotide polymorphisms (SNPs). We then impute the masked genotypes in the study sample by using either the most diverse reference panel or by using randomly selected reference panels. We also apply the “most diverse” method to sequences of European ancestry from the 1000 Genomes Project. The results from both the simulated sequences and the 1000 Genomes sequences show that the most diverse reference panel consistently provides higher imputation accuracy, independent of imputation lengths, reference panel sizes, and marker densities in the study sample. We thus provide a cost-effective strategy for designing sequencing studies for samples with existing genome-wide genotype data. As of 2013, thousands of GWAS have been performed, with over one million genotyped individuals (http://www.genome.gov/gwastudies/). Effective use of the genotype data will make it possible to carry out large-scale sequencing studies on these individuals *in silico* with a limited budget.

3.2 Materials and methods

3.2.1 Phylogenetic diversity

We use notation similar to that of Steel (2005). Assume a study sample T of n haploid individuals, each containing q polymorphic sites that are genotyped for $k < q$ variable sites (referred to as markers) in a region of interest. We consider haploid data (phased diploid individuals for humans), as we do not focus on phasing. Based on the genotypes at those k markers, we aim to identify a subset $S \subset T$ of size $m \leq n$ to be sequenced. Sequencing reveals $r \leq q$ - k additional variable sites in the m individuals. S is then used as a reference panel to impute the genotypes of these r sites in the remaining n - m individuals in the study sample T.

To identify the optimal selection of S, let X_T be an unrooted tree constructed using all haplotypes in T on the basis of the k markers. Let λ_T be the sum of the branch lengths for all edges of X_T. We denote by X_S the induced tree obtained by restricting X_T to only the haplotypes in S and by λ_S the sum of the branch lengths of X_S. For $m \geq 2$, we define the size-m subset of T with maximal phylogenetic diversity as pd_m:

$$pd_m = \text{arg max}\{\lambda_S : S \subseteq T \text{ and } |S| = m\}.$$

3.2.2 Identifying the subset with maximal diversity

To find pd_m, we first generate an unrooted tree from the study sample T. Based on the genotypes of the k markers, we compute the Hamming distances between individual haplotypes and construct a pairwise distance matrix for *T*. Based on this distance matrix, we construct a tree using the neighbor-joining method, which recursively agglomerates pairs of nodes until all nodes have been incorporated into the tree (Saitou and Nei 1987). On this tree, we apply a greedy algorithm to identify the subset *S* with size *m* that has the maximal phylogenetic diversity. Briefly, we first select the pair of haplotypes with the greatest distance on the tree and add the pair to *S*. We then sequentially incorporate as the next haplotype in *S* the haplotype that adds the maximal length to the chosen tree at that step, repeating the process until *S* reaches size *m*. Pardi and Goldman (2005) and Steel (2005) proved that conditional on the tree, the subset chosen according to this greedy algorithm has the maximal phylogenetic diversity.

3.2.3 Simulations

We analyze simulated datasets to evaluate the performance of the "most diverse reference panel" in genotype imputation. We independently generate 50 datasets of 2000 haplotypes each with the program *ms*, a coalescent-based sequence sampling program, under the neutral Wright-Fisher model (Hudson 2002). We assume a basic population-genetic model with constant effective population size N_e = 10,000, a mutation rate μ = 1.0^{-8} per site per generation, and a recombination rate ρ = 1.0^{-8} per site per generation. We remove singletons from the simulated sequences to create the "true" imputable sequence data. All simulated sites are assumed to have at most two alleles. Emulating the density of current genotype arrays, we select the marker panel of the study sample (the "genotype data") by randomly choosing 300 markers per Mb that have MAF > 0.1 in the sequence data. We mask the genotypes for the remaining sites, which become the set of sites that will be imputed. We simulate haplotypes of length 1 Mb, imputing the middle

100 kb while keeping the genotypes for the marker panel in both 450-kb flanking regions to improve imputation accuracy and to avoid edge effects (Li et al. 2010). Based on these simulated marker genotype datasets, we apply our algorithm on the marker panel to obtain the most diverse reference panels of 200 haplotypes. To evaluate the performance of the most diverse reference panel, for each of the 50 simulated datasets, we generate 1000 random reference panels, by sampling without replacement 200 haplotypes each from the sequence data for comparison. We ignore the pairing status of two haplotypes in a diploid individual when selecting the most diverse panel. In practice we can not only sequence one chromosome in a diploid individual. To incorporate this more realistic case, we consider the pairing status in diploid case and form the "diverse diploid panel". If we plan to sequence 100 diploid individuals out of 1000 diploid individuals, we form the diverse diploid panel by continuing to incorporate diploid individuals who carry one or two haplotypes into the panel from the top diversity list until we reach 100 diploid individuals. In each reference panel, we unmask all imputable sites and use the resulting sequences as references for genotype imputations. For each dataset, we perform one imputation with the most diverse reference panel, one imputation with the diverse diploid reference panel, and one imputation with each of the 1000 randomly selected reference panels.

To evaluate the impact of our parameter choices, we modify this basic design by changing the length of the imputation target, the reference panel size, and the number of genotyped SNPs in a study sample while maintaining the other parameters fixed as described above. We consider imputation target lengths of 100 kb, 500 kb, 1 Mb, and 2

Mb, each time adding 450 kb flanking regions. We select reference panel sizes of 100, 200, 300, 400, and 500 haplotypes among a total of 2000 haplotypes. We also vary the number of genotyped markers from 300 to 1000 in a 1 Mb region in a study sample. For each scenario, we simulate 50 datasets of 2000 haplotypes each. For each dataset, we perform one imputation with the most diverse reference panel and 50 imputations with randomly selected reference panels.

Based on previous comparisons among imputation methods (Hao et al. 2009; Nothnagel et al. 2009; Pei et al. 2010), we employ *minimac* (Howie et al. 2012) as one of the best-performing methods. This method is an extension of MaCH (Li et al. 2010) for phased diploid data. To assess imputation accuracy on heterozygous genotypes, we then create *n*/2 diploid individuals by randomly combining pairs of haplotypes from the entire study sample. After imputation, we evaluate the predicted imputation accuracy by examining for each selected reference panel the mean of the estimated correlation coefficient $\hat{\mathrm{r}}^2$ across all markers. To evaluate the imputation accuracy of the r imputed sites for the *n*/2 diploid individuals in the imputed datasets, we compute two measures for the discordance rate between the imputed genotypes $\hat{g}_{ij}$ and the simulated genotypes g_{ij} at variant site *j* in target individual i. We let $\hat{g}_{ij}$ and g_{ij} equal to 0, 1 and 2, based on their numbers of copies of one specific allele. First we calculate discordance rate D across all sites:

$$\mathrm{D} = \frac{\sum_{\mathrm{i=1}}^{\mathrm{n/2}} \sum_{\mathrm{j=1}}^{\mathrm{r}} |g_{ij} - \hat{g}_{ij}|}{nr}.$$

As this error function is strongly affected by the minor allele frequencies of the variant sites examined (Huang et al. 2009), we also calculate imputation errors across all heterozygous genotypes ($g_{ij} = 1$):

$$\mathrm{H} = \frac{\sum_{\mathrm{i}=1}^{\mathrm{n}/2} \sum_{\mathrm{j}=1}^{\mathrm{r}} 1_{g_{ij}=1} |g_{ij} - \hat{g}_{ij}|}{2 \sum_{\mathrm{i}=1}^{\mathrm{n}/2} \sum_{\mathrm{j}=1}^{\mathrm{r}} 1_{g_{ij}=1}}.$$

3.2.4 The 1000 Genomes Project data

We apply our method to sequence data from the 1000 Genomes Project. We consider the phased data of 381 diploid individuals (762 haplotypes) with EUR (European) ancestry, including 87 CEU (Utah residents with Northern and Western European ancestry), 93 FIN (Finnish from Finland), 89 GBR (British from England and Scotland), 14 IBS (Iberian populations in Spain), and 98 TSI (Toscani in Italy) (http://www.sph.umich.edu/csg/abecasis/MACH/download/1000G-PhaseI-Interim.html, the 1000G Interim Phase I Haplotypes 11/23/2010 release). We remove singletons from the sample, selecting eight 100-kb regions that are approximately evenly distributed across chromosome 20. We create study samples using a similar procedure as the simulation above: for each region, we add a 450-kb flanking region on each side, randomly choose ~300 genotyped SNPs per Mb among markers with MAF ≥ 0.1, and mask the genotypes of all other sites. In each region, we select the most diverse 160 haplotypes from the set of 762 total haplotypes as the diverse reference panel. For comparison, we sample without replacement 1000 random reference panels of 160 haplotypes each.

We next consider the entire chromosome 20 and create a study sample using the same procedure as in the 100 kb regions. We select the most diverse reference panel using our method and 50 reference panels randomly without replacement. Using the selected reference panels, we impute all the masked genotypes and compute the discordance rate for each imputation.

3.3 Results

3.3.1 Number of imputed sites

Polymorphic sites in reference panels: Only sites that are polymorphic in the reference panel can be imputed into the remaining study sample. Hence, we first evaluate the number of polymorphic sites in the reference panels selected. For each of the 50 simulated datasets, we choose one random reference panel and compare it to the most diverse reference panel. We find that for a total of 12,957 masked sites that are polymorphic in the study samples across the 50 datasets, 9,642 of sites (74.41%) are polymorphic in both types of reference panels. Among the remaining sites, 1,492 sites (11.52%) are polymorphic only in the most diverse reference panels, whereas 760 sites (5.87%) are polymorphic only in the randomly selected reference panels. Thus, on average, 5.65% more sites are polymorphic in the most diverse reference panels than in the randomly selected reference panels.

Polymorphic sites in imputed datasets: To ensure that the higher number of polymorphic sites in the most diverse reference panels also leads to a higher number of imputed polymorphic variants, we count the number of imputed sites that are polymorphic in datasets imputed with reference panels generated under three different selection strategies: (1) sampled at random, (2) selecting the 200 most diverse haplotypes and (3) selecting the diverse considering the haplotype pairing status (diverse diploid reference panel). As it is not currently practical to sequence only one chromosome in a diploid organism, strategy (3) represents a scenario in which the individuals that carry the most diverse haplotypes are identified and both of their chromosomes are sequenced. Across the 50 datasets, the mean number of haplotypes that one diverse diploid panel of 200 incorporates from the top diversity list is 106, ranging from 102 to 112. Assuming Hardy-Weinberg equilibrium, this second chromosome is sampled randomly from the population.

From the total of 12,957 imputed sites across the 50 datasets, 10,952 are polymorphic in datasets imputed with the most diverse reference panels (84.53%), 10,574 are polymorphic for the diverse diploid reference panels (81.61%), and 10,151 are polymorphic for randomly selected reference panels (78.34%). **Figure 3.2** shows percentages of polymorphic sites in datasets imputed with the three reference types across the 50 datasets. In each of the 50 datasets, imputation with the most diverse reference panel captures more polymorphic sites than imputation with the random reference panel. The improvement by using the most diverse panel is greater when the randomly selected panel captures only a low percentage of polymorphic sites (e.g., replicates 46 to 50). Imputations with the diverse diploid panels result in higher percentages of polymorphic sites than the random panels in 42 of the 50 datasets (84%) and in a higher percentage of polymorphic sites than the most diverse panel in 4 of the 50 datasets (8%). Only in four datasets does the random reference panel perform substantially better than the diverse diploid reference panel (replicate 1, 2, 3, and 6) and in all these cases, the random panel captures a high (> 83%) percentage of polymorphic sites.

3.3.2 Imputation accuracy

As a measurement of imputation accuracy, we evaluate the discordance rate between the simulated genotypes and the imputed genotypes for the 50 simulated datasets. For each dataset, we compare the accuracy of the imputation using the most diverse reference panel to the empirical distribution of imputation accuracies from 1,000 random reference panels.

Estimated imputation quality: A predictor for the accuracy of an imputed site generated by *minimac* is the $\hat{r}^2$, a quantity calculated by comparing the variance of observed genotype scores with the variance of expected genotype scores to estimate the squared correlation at a marker between the true allele counts and the estimated allele counts (Li et al. 2010). To compare this predicted imputation accuracy between the different choices of reference panels we compute the average $\hat{r}^2$ across the 12,957 total imputed sites across the 50 datasets. For imputations with the most diverse reference panels and the diverse diploid reference panels, we generate one value of $\hat{r}^2$ for each site; to evaluate imputations with the 1000 randomly selected reference panels for each dataset, we compute the mean $\hat{r}^2$ for each site across 1000 imputations, and we then calculate the average across all imputed sites. Sites imputed with the most diverse reference panels have the highest mean $\hat{r}^2$ (0.784), followed by sites imputed with the diverse diploid reference panels (0.758). Sites imputed with randomly selected reference panels have the lowest mean $\hat{r}^2$ (0.723). As removing variant sites with $\hat{r}^2 < 0.3$ filters most poorly imputed sites (Li et al. 2009), we also compare the number of sites that pass this imputation quality threshold. Across the 50 datasets, we observe that a higher percentage of sites imputed with the most diverse reference panels pass the threshold (83.17%) compared to sites imputed with the diverse diploid reference panels (80.53%) and sites imputed with the randomly selected panels (77.48%). For a higher $\hat{r}^2$ threshold of 0.8 applied by typical association studies, 76.63% of sites pass the threshold for imputations with the most diverse reference panels, 74.76% for the diverse diploid reference panels, and 59.65% for the randomly selected reference panels.

Discordance rates: For each simulated dataset, we separately calculate discordance rates for all sites imputed with the most diverse reference panel, sites imputed with the diverse diploid reference panel, and the mean values for sites imputed with random reference panels taken across all 1000 random panels. Using the most diverse reference panel results in the lowest mean discordance rate across the 50 replicates (0.0019), followed by imputation with the diverse diploid reference panel (0.0022). Both quantities are lower than the mean discordance rates of imputation with the random reference panels (0.0031) (**Figure 3.3**). Ranking the discordance rate of selected reference panels together with the discordance rates of 1000 random panels from the lowest to the highest value, the most diverse reference panel is a clear outlier for 24 of the 50 datasets (48%), having a lower discordance rate than imputations with all 1000 randomly selected reference panels (rank 1). Across all 50 datasets, the mean rank of the most diverse reference panel is 13.5, ranging from 1 to 135 among 1001 panels. Across the same 50 datasets, the mean rank of the diverse diploid reference panel is 111.9, ranging from 1 to 906 among 1001 panels.

To generate a more meaningful discordance measure for low-frequency variants, we also compare the imputed genotypes and the simulated true genotypes across sites for which the true genotypes are heterozygotes. While the heterozygote discordance rate is higher than the overall discordance rate, the mean heterozygote discordance across the 50 replicates is again the lowest for sites imputed with the most diverse reference panels (0.0097), followed by the diverse diploid reference panels (0.0121) and the random reference panels (0.0165). Comparing across frequency bins, we observe that for all reference selection strategies, the heterozygote discordance rate decreases with increasing allele frequency. The mean heterozygote discordance rate across the 50 replicates for low-frequency variant sites ($0 < \text{MAF} < 0.1$) is considerably higher than the overall mean discordance rate for all heterozygote sites across the 50 replicates (0.0258 for the most diverse reference panels, 0.0329 for the diverse diploid reference panels, and 0.0415 for the random reference panels). In all frequency bins, considering heterozygote discordance rates, imputations with the most diverse reference panels generate the lowest discordance rates and imputations with the randomly selected reference panels generate the highest discordance rates, while imputations with the diverse diploid reference panels generate intermediate discordance rates (**Figure 3.3**). Combining the heterozygote discordance rate of the most diverse reference panel with the heterozygote discordance rates of 1000 random panels for each of the 50 simulated datasets and ranking from the lowest to the highest heterozygote discordance rate, the mean rank of the most diverse panel across all 50 datasets is 17.5 when comparing all heterozygote sites, 27.3 for sites with $0 < \text{MAF} < 0.1$, 115.7 for sites with $0.1 \leq \text{MAF} < 0.2$, and 68.5 for sites with $0.2 \leq \text{MAF} \leq 0.5$ out of

1001 panels ranked. When comparing the diverse diploid reference panel to random panels, the mean rank across all 50 datasets is 147.9 for all heterozygote sites, 188 for sites with 0 < MAF < 0.1, 163.9 for sites with 0.1 ≤ MAF < 0.2, and 145.9 for sites with 0.2 ≤ MAF ≤ 0.5.

3.3.3 Imputation accuracy under different simulation settings

To assess the robustness of our results, we evaluate the performance of the most diverse reference panel under different simulation settings, considering different target sequence lengths, different reference panel sizes, and different marker densities in the study sample. We first investigate whether the lengths of the target regions affect the performance of the most diverse reference panels in imputations. We impute regions with lengths of 100 kb, 500 kb, 1 Mb and 2 Mb, using both the most diverse reference panel and 50 random reference panels, each of which is compared to the true underlying genotypes; the average of the 50 discordance rates is then compared with the discordance rate for the most diverse reference panel. As shown in **Figure 3.4a**, across the four different lengths, we observe little effect of the imputation length on the discordance rate. The mean discordance rate across the 50 replicates for each group ranges from 0.0028 (2 Mb) to 0.0037 (500 kb) for the most diverse reference panel and from 0.0052 (2 Mb) to 0.0058 (100 kb) for the random reference panels. For all sequence lengths considered, the most diverse reference panels provide lower discordance rates than the randomly selected reference panels.

Second, we evaluate how the reference panel sizes affect the performance of the most diverse reference panel by comparing the genotype discordance rates for reference panels of size 100, 200, 300, 400, and 500 haplotypes. For both reference panels, the mean discordance rate across the 50 replicates decreases with larger reference panel sizes, from 0.008 to 0.0006 for the most diverse panel and from 0.009 to 0.0015 for the random reference panels. Especially for a reference panel of size 100 individuals, the discordance rate is considerably higher than for larger panel sizes. Across all reference panel sizes, imputations with the most diverse reference panels consistently provide lower discordance rates than do imputations with the randomly selected reference panels (**Figure 3.4b**).

Third, we examine how the number of markers genotyped initially in the study sample affects the performance of the most diverse reference panel by varying the density of markers in the study sample, considering 200, 300, 400, 500, 600, and 1000 markers per 1 Mb region. For both types of reference panels, the mean discordance rate across the 50 replicates decreases with a higher density of markers in the study samples, from 0.0055 to 0.0015 for the most diverse panel and from 0.0072 to 0.0023 for the random reference panels. Across all marker densities in the study sample, the most diverse reference panels consistently provide lower discordance rates than the randomly selected reference panels (**Figure 3.4c)**. We also observe that the improvement in discordance rates for the most diverse reference panel over the randomly selected panels slightly decreases with more markers genotyped in the study sample.

3.3.4 Imputation accuracy on data from the 1000 Genomes Project

We apply our method to real sequence data of 381 phased individuals with EUR ancestry from the 1000 Genomes Project. Considering eight 100-kb regions across chromosome 20, we impute 3,215 sites after removing singletons. Sites imputed with the most diverse reference panels have a mean $\hat{r}^2$ of 0.749 across sites; sites imputed with the 1000 randomly selected reference panels have a mean $\hat{r}^2$ of 0.741. Slightly more sites pass the imputation quality threshold of $\hat{r}^2 \geq 0.3$ for the most diverse reference panels (85.75%) than for the randomly selected reference panels (84.23%). When applying a higher imputation threshold of $\hat{r}^2 \geq 0.8$, a similar percentage of sites pass the threshold for the most diverse reference panels (62.74%) and the randomly selected reference panels (62.89%).

Considering all imputed sites for the eight 100-kb regions, the most diverse reference panels result in a lower mean discordance rate across the eight regions (0.0067) than the randomly selected reference panels (0.0077). When comparing imputed sites that are heterozygotes in real sequenced datasets, sites imputed with the most diverse reference panels have a lower mean discordance rate across the eight regions (0.0228) than sites imputed with the randomly selected reference panels (0.0262). The lower discordance rates from the most diverse reference panels are observed across all frequency bins for heterozygote sites: For sites with $0 < \text{MAF} < 0.1$, the mean discordance rate across the eight regions is 0.074 using the most diverse reference panels versus 0.0895 using random reference panels, for sites with $0.1 \leq \text{MAF} < 0.2$, the mean discordance rate across the eight regions is 0.0177 versus 0.0193, and for sites with $0.2 \leq \text{MAF} \leq 0.5$, the mean discordance rate across the eight regions is 0.0080 versus 0.0099 (**Figure 3.5**). However, we also notice that the performance of the most diverse reference panel varies widely among the eight regions. When ranking the discordance rate of the imputation by the most diverse reference panel with the discordance rates of the 1000 imputations by randomly selected reference panels from the lowest to the highest value for each of the eight regions, the most diverse reference panel has an average rank of 116.1 across the eight regions, ranging from 3 to 496 out of 1001 panels ranked. For heterozygote sites, the most diverse reference panel has an average rank of 156.7, ranging from 1 to 508; for heterozygotes in different MAF bins, the most diverse reference panel has an average rank of 242.7 for sites with $0 < MAF < 0.1$, an average rank of 311.0 for sites with $0.1 \leq MAF < 0.2$, and an average rank of 129.4 for sites with $0.2 \leq MAF \leq 0.5$ out of 1001 panels ranked.

For the whole chromosome 20 data, the sequence dataset contains 259,618 sites after removing singletons. We select 18,000 sites with $MAF \geq 0.1$ as “genotyped” markers and mask the genotypes for the remaining 241,618 sites to create a study sample. Based on the genotyped markers, we select the most diverse reference panel to impute the genotypes of the masked sites. For comparison, we sample 50 reference panels at random. We first compare the number of masked sites that are polymorphic in the selected reference panels. In the most diverse reference panel, 211,480 masked sites are polymorphic (87.53%), compared to an average of 210,137 across the 50 random reference panels (86.97%). After imputation, we observe that the imputation with the most diverse reference panel has 201,831 sites with $\hat{r}^2 \geq 0.3$ (83.53%), whereas 200,609 sites have mean $\hat{r}^2 \geq 0.3$ with a randomly selected reference panel (83.03%). For the higher imputation quality threshold of $\hat{r}^2 \geq 0.8$, 142,996 sites pass the threshold for the imputation with the most diverse reference panel (59.18%), whereas averaging 142,281 sites across imputations with the 50 randomly selected reference panels pass the threshold (58.89%). Moreover, sites are imputed slightly more accurately with the most diverse reference panel than with random reference panels (**Table 3.1**). The discordance rate of the most diverse panel is lower than all except 2 of the 50 random panels (rank 3). To evaluate the imputation accuracy in different frequency bins, we again consider discordance rates of heterozygote genotypes. When ranking the discordance rate of the imputation by the most diverse reference panel with the discordance rates of the 50 imputations by randomly selected reference panels from the lowest to the highest value, we observe that the most diverse reference panel has a lower discordance rate than all 50 random panels (rank 1). Examining separate frequency bins, the most diverse reference panel has rank 4 for sites with $0 < \text{MAF} < 0.1$, rank 3 for sites with $0.1 \leq \text{MAF} < 0.2$, and rank 14 for sites with $0.2 \leq \text{MAF} \leq 0.5$. Averaging across sites, the numerical improvement in imputation accuracy by using the most diverse panel is modest, reducing imputation errors by 1% across all sites and by 2.3% at less common variants with $0 < \text{MAF} < 0.1$.

3.4 Discussion

The cost reduction in modern sequencing technology enables investigators to generate a reference panel for genotype imputation by sequencing a subset of the study sample. We have proposed a sampling strategy for such an internal reference panel by adapting an algorithm based on phylogenetic diversity. In simulated sequence data, our method consistently outperforms randomly selected reference panels, in that it provides higher imputation accuracy and recovers more polymorphic sites from the sample. This improved performance holds across different imputation lengths, different reference panel sizes, and different marker densities in the study sample. Upon analyzing real sequence data with European ancestry from the 1000 Genomes Project, the most diverse reference panel provides higher imputation accuracy than do randomly selected reference panels. We observe this improved performance when imputing eight 100-kb regions on chromosome 20 and when imputing the entire chromosome 20, indicating that our method can be used to select reference individuals for imputing smaller target regions as well as for imputing entire genomes. Our method may be particularly advantageous for imputing less common variants, as we found in our simulations that the most diverse reference panels have more polymorphic sites than do randomly selected reference panels. Moreover, the accuracy gain from using the most diverse reference panel instead of randomly selected reference panels is greater for less common variants (e.g., $0 < MAF < 0.2$) than for more common variants (e.g., $MAF \geq 0.2$) (**Table 3.1**).

Our method is fundamentally different to Pasaniuc (2010). Although both selections are based on the genotypes of makers that exist in the study sample and reference sequences, we adapt phylogenetic diversity in our method whereas Pasaniuc and colleague’s method identifies one different reference panel for each short window (e.g., 15 kb) of the target region for each study individual based on coalescent theory. In addition, their method requires having a pool of sequences to select from. This is not the case for our purpose as we don’t have all the sequences and can only sequence a subset of the study sample.

Kang and Marjoram (2012) very recently considered sample selection for next-generation sequencing using a similar approach based on maximizing the subtree length. Compared to our NJ method, Kang and Marjoram used the UPGMA tree. In general, the NJ method is more accurate in computing branch lengths as it considers all taxa on the tree when estimating branch lengths whereas UPGMA only select the closest neighbors and compute the arithmetic mean. In addition, Bryant (2005) proved the NJ is statistically consistent given the distance data whereas UPGMA does not always satisfy the consistency criteria. Finally, UPGMA requires the ultrametric condition, the final tree is a clock-like tree and each individual on the tree has the same distance to the root. As a result, we expect the method based on UPGMA to have more ties that evolve sample uniformly at random in selecting a subset with maximal tree length than our method as our NJ tree does not require the ultrametric assumption. Although they have used a different tree-building algorithm, they examined a similar greedy method, motivated by coalescent theory instead of from the standpoint of phylogenetic diversity. In simulations that examined different marker densities, target imputation region lengths, and reference panel sizes, they found that their algorithm performed well, and we similarly find that our related method performs well under these scenarios. In addition, the work of Pardi and Goldman (2005) and Steel (2005) provides further theoretical justification for the basis of our algorithm, as well as for the method of Kang and Marjoram. Taken together, our study and that of Kang and Marjoram demonstrate the value of sensible use of genealogical relationships among samples to improve the experimental design for sequencing studies. Further, as shown in Pardi and Goldman (2005), our method can incorporate other selection criteria by starting with an initial selection of haplotypes and then applying the greedy algorithm as an extension.

We expect that the most diverse reference panel algorithm can work effectively either on a limited region of the genome or on whole chromosomes, provided the phylogenetic tree based on existing data reasonably captures the ancestral relatedness of the haplotypes in the study sample. This is only possible if this ancestral relatedness can be described well as a tree, a condition that depends on the population-genetic history of the sample and the size of the region of interest. When focusing on a single genomic region, relevant parts of its ancestral process can be approximated as a tree due to limited recombination events. This single tree can be estimated by a subset of genotyped markers, and thus, our method can provide useful information for reference panel selection. On the other hand, many uncorrelated trees can be formed to represent the ancestral processes of a large region such as the entire genome. Hence, an approximation with a single tree might not capture many features of the data. In such a scenario, it is less likely that our method will produce a better reference panel than a random sample. In a structured population, the underlying population structure generates a correlation of ancestries across the entire genome. The resulting clades can be approximated by the tree-building algorithm, and this tree can help in selecting a more diverse reference panel. It is encouraging that in a sample of five European subpopulations, the population structure was sufficient for the most diverse reference panel selected based on the entire chromosome 20 to outperform the randomly selected reference panels. Hence, relatively subtle population structure, such as that found in samples from closely related European countries, is sufficient to create similarities in the underlying ancestral processes that can be captured by the tree-building algorithm and can result in improved reference panel selection. For subpopulations with different sample sizes, we expect the diverse algorithm only oversample from subpopulations with many individuals that have dramatic longer external branch lengths that individuals from other subpopulations on the constructed tree, or undersample in the case of dramatic short external branch lengths. Otherwise, we expect our algorithm will pick the number of individuals that are proportional to the size of each subpopulation.

Our method is based on local phylogenetic tree. The topology of the local phylogenetic tree may change with increasing size of a genome region because of recombination events. As the performance of our method is based on how well the local phylogenetic tree approximates the ancestral relatedness of the study individuals, we expect the gain in imputation accuracy using our method will decrease with increasing length of an imputation region. As expected, the average improvement in imputation accuracy when imputing 100-kb regions is considerably higher than the average improvement across the entire chromosome, reflecting that the ancestry of a 100-kb region is more tree-like than the ancestry of an entire chromosome. However, the average improvement in imputation accuracy when imputing 100-kb regions is considerably higher than the average improvement across the entire chromosome, reflecting that the ancestry of a 100-kb region is more tree-like than the ancestry of an entire chromosome.

The method of reference panel selection described here can be adapted to address specific study design goals. Our method can be applied to incorporate other criteria in reference panel selection. For example, we have not specifically incorporated phenotype information when selecting reference haplotypes, so the selected reference panel is not guaranteed to include the individuals with traits of interest. To sequence certain individuals because of their phenotypes or other criteria unrelated to their phylogenetic placement, we can apply the selection algorithm conditional on including these individuals in the reference panel. The greedy algorithm still guarantees that the subsequent extension has optimal phylogenetic diversity, as proved in Pardi and Goldman (2005). Similarly, our method can be easily extended to form a reference panel by incorporating sequences partly from the study sample and partly from an external database such as the HapMap Project or the 1000 Genomes Project. For example, we can treat sequences from the HapMap Project as an initial set and apply the greedy algorithm to the study sample as an extension in a similar manner as in analyses treating other inclusion criteria.

Our method should be applicable to imputation in other species of a genome region in other species as long as the constructed tree can reasonably represent the ancestral relatedness among the study individuals. Wang et al. (2012) proposed to use local phylogenetic tree to provide confidence information in imputing sequences in inbred mice. The confidence is high for imputing study strains that share one or more genome intervals with reference sequences, whereas the confidence is low for strains that do not share genome intervals with reference sequences. The authors also proposed that sequencing these strains with low confidence imputation quality could provide maximal improvement in imputation accuracy and new variant identification. The strategy used by

Wang et al (2012) may work well as an extension to our study to combine existing sequence data in imputation. For example, to get the full sequences of a genome region for a study sample, we can form a reference panel from the 1000 Genomes Project that share one or more haplotypes with our study sample and impute the sequences of the these study individuals with high confidence, and apply the our method to the rest of study individuals or sequencing all the rest of study individuals if budget allows.

In summary, we have demonstrated that an innovative method of choosing an internal reference panel — the most diverse reference panel — can be a cost-effective approach for planning sequencing studies with existing genotype array data. The method can readily incorporate a variety of selection criteria, while still guaranteeing the maximal phylogenetic diversity for subsequent selections.

Table 3.1 Discordance rates for imputations for real sequencing data. Data are from chromosome 20 of individuals with European ancestry in the 1000 Genomes Project. Discordance rates are shown as percentages. We split 381 phased diploid individuals into a target sample of 301 target individuals and a reference panel of 160 haplotypes. Shown here are results from one imputation with the most diverse reference panel and the mean and standard deviation of the discordance rates from 50 imputations with randomly selected reference panels. We ranked discordance rates of the most diverse panel together with 50 random reference panels from the lowest to the highest value and display the rank of the most diverse panel.

Reference types		Variant groups				
		All	Heterozygotes	MAF(0,0.1)	MAF[0.1,0.2)	MAF[0.2,0.5]
Most diverse		1.02	3.53	10.31	2.77	1.92
Random	mean	1.03	3.57	10.45	2.82	1.93
	standard deviation	0.004	0.019	0.076	0.019	0.014
Rank of the most diverse		3	1	4	3	14

Figure 3.1 Illustration of the selection of the most phylogenetically diverse reference panel. Shown is the phylogenetic tree constructed from 20 simulated haplotypes as well as the most diverse subset of five taxa (in bold). The selection algorithm first selects the most distant pair of taxa and then identifies haplotypes that are most distant conditional on the haplotypes already selected. To choose the five taxa, the greedy algorithm first selects pair 1 and 14, and then 12, 19, and 5 sequentially. Notice how the haplotypes chosen are spread across the tree and possess long branch lengths.

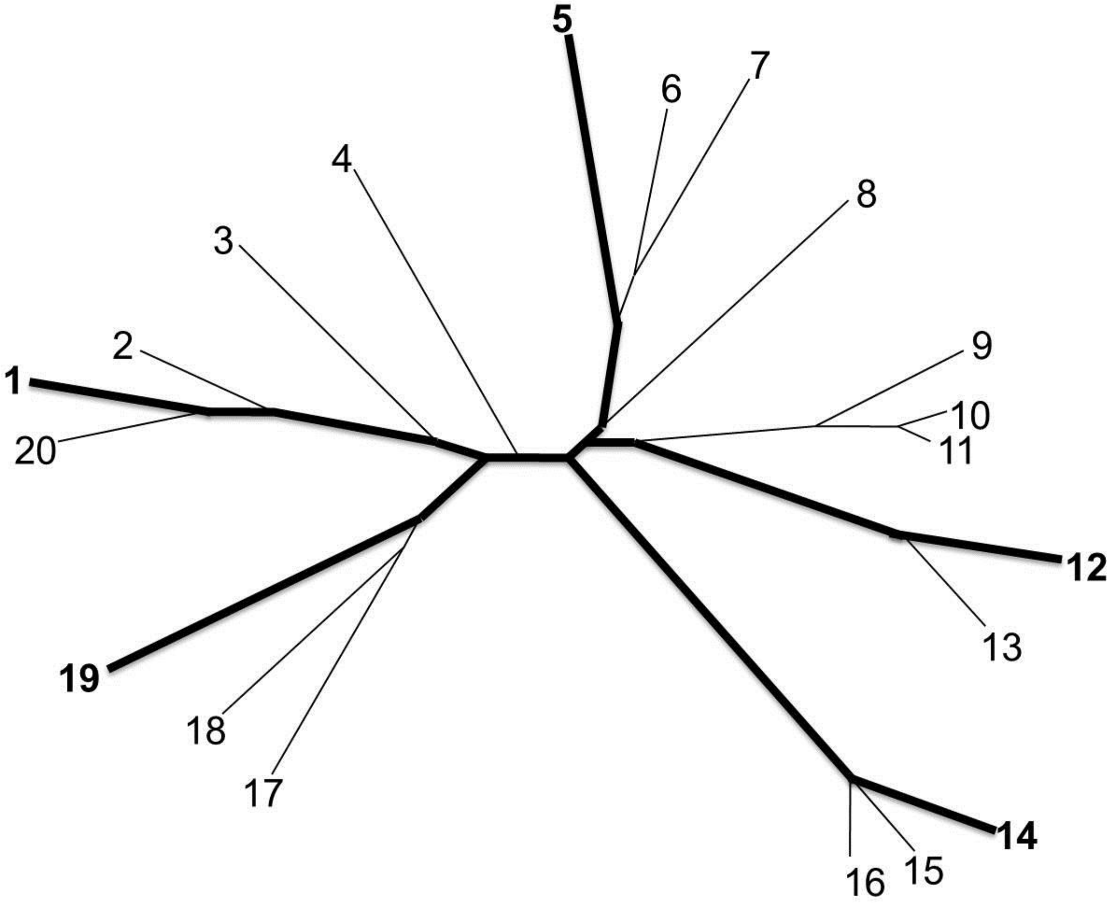

Figure 3.2 Percentages of polymorphic sites in imputed datasets. The white bar represents the accuracy of a random panel, the grey bar represents the accuracy of the diverse diploid panel, and the black bar represents the accuracy of the most diverse reference panel. If the performance of the diverse diploid reference panel is lower than the performance of the random reference panel, this difference is indicated by the part of the white bar with horizontal stripes. If the accuracy of the diverse diploid panel is higher than the accuracy of the most diverse panel, this difference is indicated by the part of the grey bar with vertical stripes. Data are 50 imputed datasets that are sorted in decreasing order by percentage of polymorphic sites recovered by imputations with random reference panels.

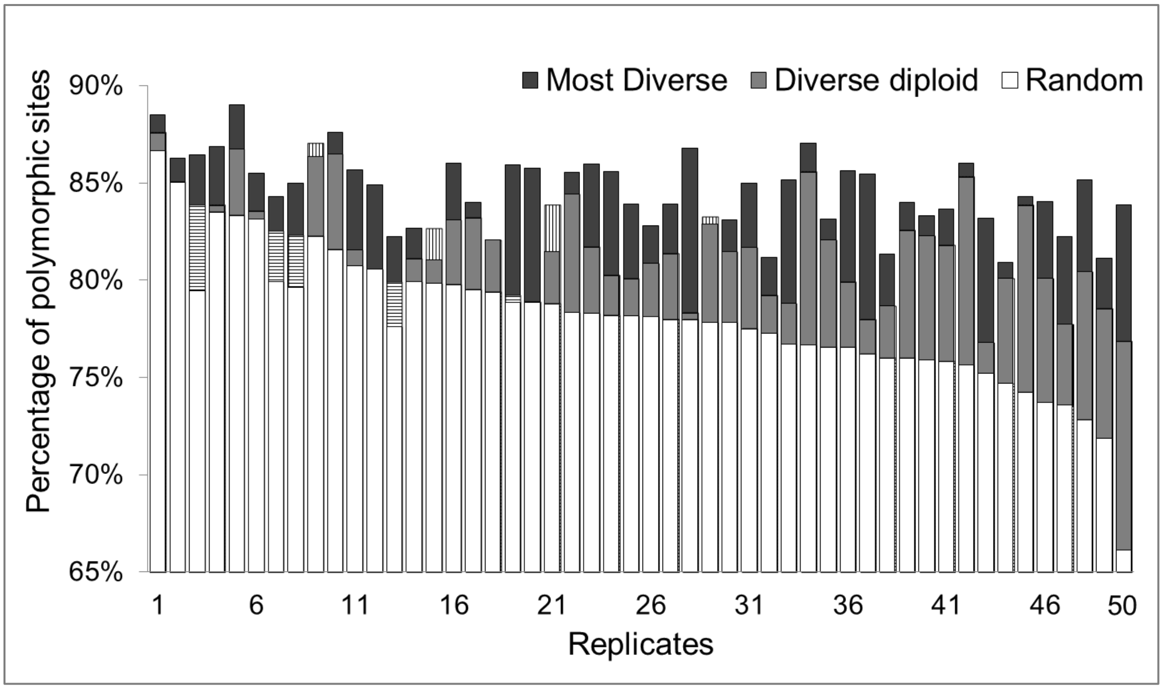

Figure 3.3 Comparison of imputation accuracy. Boxplots of discordance rates between imputed genotypes and simulated genotypes for imputations with randomly chosen reference panels, diverse diploid reference panels, and most diverse reference panels. The mean discordance rate across the 50 replicates for each comparison group is indicated by a diamond, and the median discordance rate across the 50 replicates for each comparison group is indicated by a middle line. The horizontal axis labels the comparison on the basis of all sites (All), all heterozygote sites (Heterozygotes), and heterozygotes in different MAF groups in the simulated sequence data.

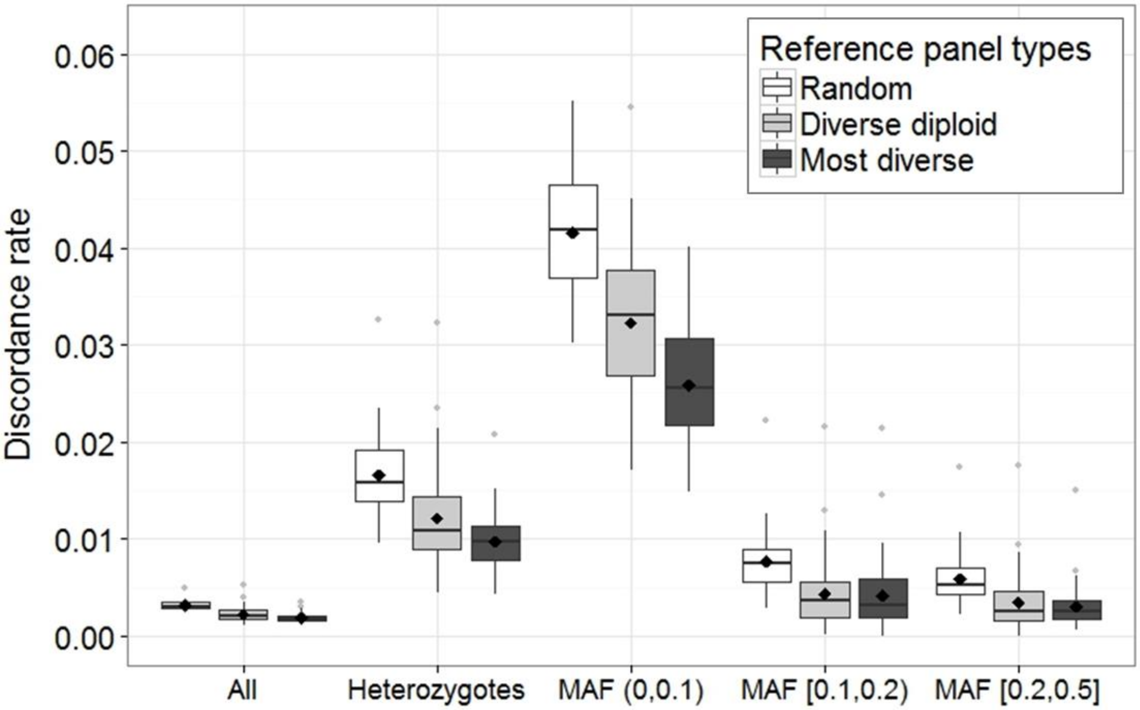

Figure 3.4 Imputation accuracy under different scenarios. Boxplots of discordance rates between imputed genotypes and simulated genotypes for imputations with randomly chosen reference panels and most diverse reference panels with varying simulation settings: A. Imputation length; B. Reference panel size; C. Number of genotyped markers per Mb in the study sample. For each dataset, we examine the mean of 50 random reference panels and the most diverse reference panel. The mean discordance rate across the 50 replicate simulated datasets for each comparison group is indicated by a diamond, and the median discordance rate is indicated by a middle line.

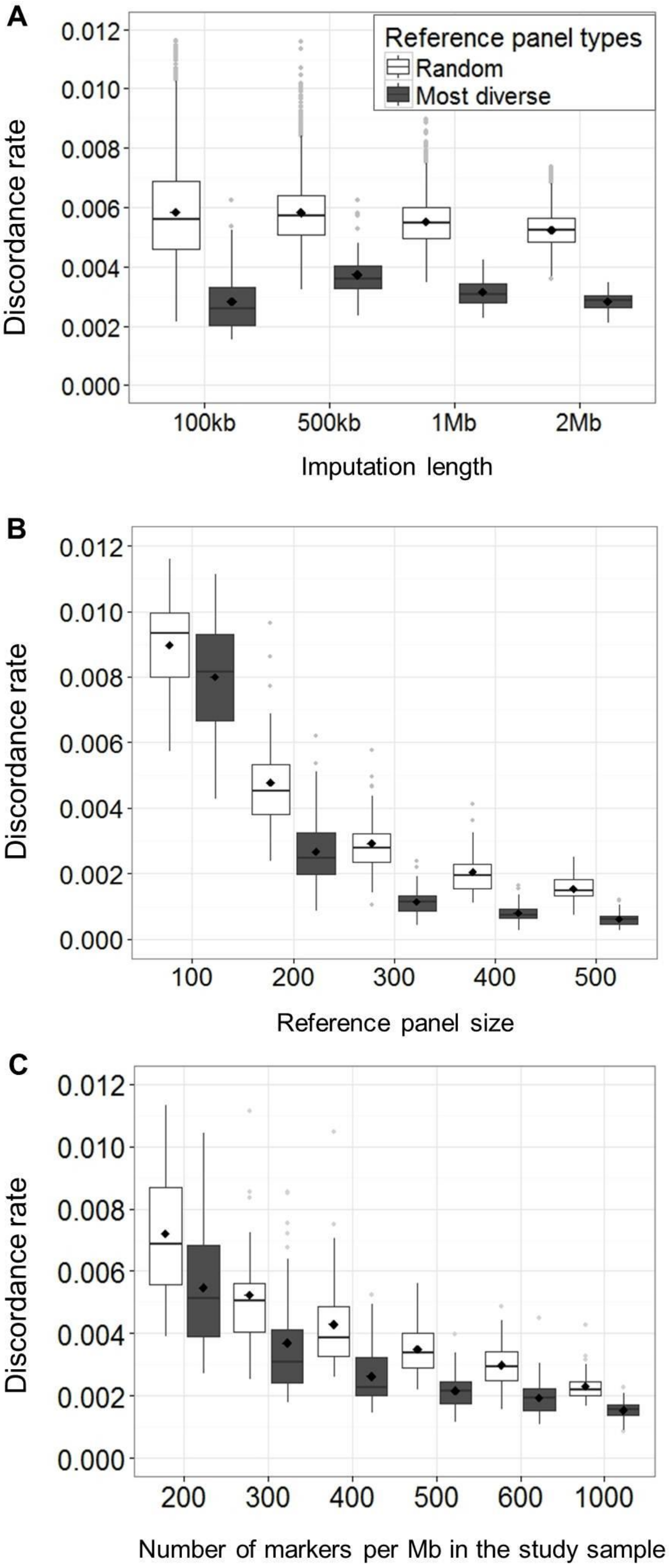
A
Reference panel types
Random
Most diverse
Discordance rate
0.012
0.010
0.008
0.006
0.004
0.002
0.000
100kb
500kb
1Mb
2Mb
Imputation length
B
Discordance rate
0.012
0.010
0.008
0.006
0.004
0.002
0.000
100
200
300
400
500
Reference panel size
C
Discordance rate
0.012
0.010
0.008
0.006
0.004
0.002
0.000
200
300
400
500
600
1000
Number of markers per Mb in the study sample

Figure 3.5 Imputation accuracy on the 1000 Genomes Project data. Boxplots of discordance rates between imputed genotypes and simulated genotypes for imputations with randomly chosen reference panels and most diverse reference panels for eight 100-kb regions on chromosome 20. We analyzed 762 haplotypes of European ancestry from the 1000 Genomes Project. The horizontal axis represents comparison of all sites (All), all heterozygote sites (Heterozygotes), and heterozygotes in different MAF groups in the simulated sequence data. The mean discordance rate across the eight regions for each comparison group is indicated by a diamond, and the median discordance rate across the eight regions for each comparison group is indicated by a middle line.

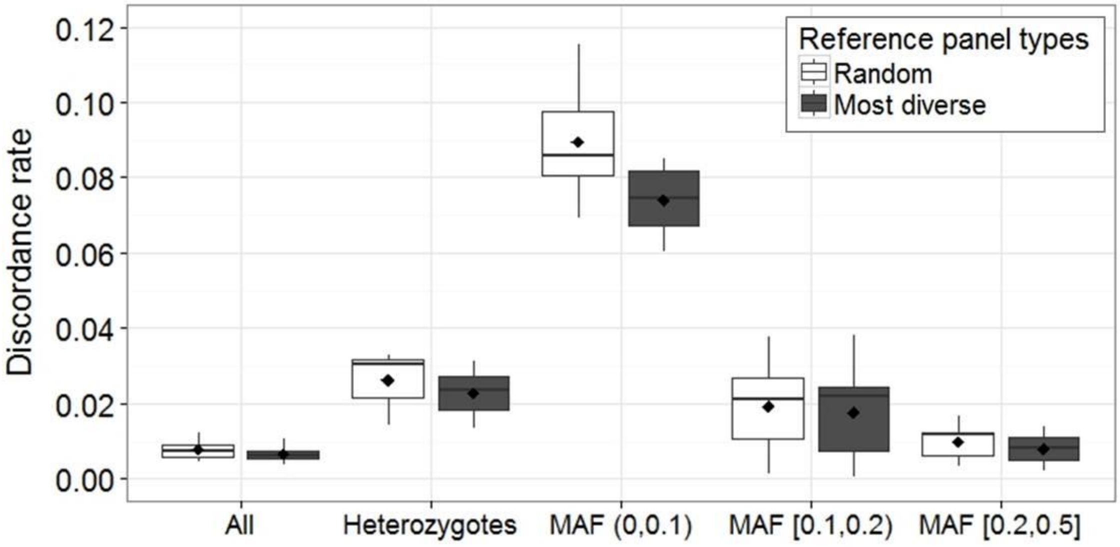

Chapter 4 Selecting the most representative sample in genotype imputation for next-generation sequencing

4.1 Introduction

Genome-wide association studies (GWAS) have successfully identified many of the common genetic variants for complex diseases. With the dramatic cost reduction in next-generation sequencing technology, investigators have begun to use sequencing studies to identify genetic risk variants for complex diseases with a focus on rare variants (Nelson et al. 2012; Xia et al. 2012). However, sequencing a large study sample is still very expensive. Thus, we need sampling strategies to select an optimal subset such that we can identify the maximal number of variable sites in the study sample and achieve the maximal imputation accuracy when imputing the sequences for the rest of the study sample using the sequenced individuals as references.

Genotype imputation is a statistical approach that predicts genotypes in a less densely typed study sample by using information from a more densely genotyped dataset as a reference panel. The most commonly used reference panels are sequences from the International HapMap Project (The International HapMap Consortium 2005) and the 1000 Genomes Project (The 1000 Genomes Project Consortium 2010). Investigators have used these sequences as reference panels to impute the genotypes for untyped HapMap markers in their GWAS. Here, we aim to identify a subset from a study sample to sequence and to use the sequenced subset as a reference panel to obtain sequences for the rest of the study sample. Sequencing can identify novel variants that are unique to a study sample. In addition, compared to imputations with reference sequences from public databases such as the International HapMap Project, imputations with reference sequences from the study sample itself avoid the possible ancestral background mismatch between the reference population and the study population.

We have proposed a sampling strategy for sequencing in Chapter 3, where we propose to sequence the subset that has maximal subtree length, a panel we term the most diverse reference panel. We show that the most diverse reference panel incorporates more polymorphic sties and provides higher imputation accuracy than a randomly selected reference panel when imputing the sequences of the rest of study sample for individuals from one population or closely related populations. Kang and Marjoram (2012) proposed another tree-based method that produced similar results. Both Kang's method and our method assume that the number of mutation events is proportional to the genealogical tree length, thus the subtree with the maximal tree length is expected to carry more mutant alleles that can be identified by sequencing and consequently to recover more variants when used as a reference panel. In addition, it assumes that selected haplotypes are spread across the tree, thus could well represent the unselected haplotypes. However, this may not be true in some cases, for example, the most diverse subset may oversample haplotypes in a cluster on the tree that vastly different while fail to sample any haplotypes in a cluster that are similar with small branch lengths (Bordewich et al. 2008). The most diverse algorithm also does not count the similarity between the selected subset and unselected subset, thus the haplotypes in the unselected subset may not represented well by the haplotypes in the selected subset.

Here we propose a subset selection method that considers both the selected subset (R) and unselected subset (U). We propose the “most representative” subset, defined by the pair (R, U) such that the summation of minimum distances over all unselected haplotypes in U to the selected subset R is the smallest among all possible choices of (R, U). Because of the combinatorial nature of this problem, it is not computationally feasible to compare all instances for a large sample. By our best knowledge, there is no such existing approach as the greedy algorithm in Chapter 3 to find such a pair (R,U). Instead, we use a local search algorithm, known as the hill-climbing search, to search for the most representative panel. The local search algorithm is not systematic, but it has two key advantages over an exhaustive search: (1) it uses very little memory – usually constant amount; and (2) it can often find reasonable solutions in large state spaces for which systematic algorithms are unsuitable (Russell and Norviq 2009). The goal is to find the global optimum or a local optimum that is a reasonable approximation of the global optimum (Selman and Gomes 2006). To increase the chance of reaching the global optimum and minimize the chance of being stuck in local optimum, we randomly start multiple times and choose the replicate that has the smallest (R, U) distance as the starting point for the hill-climbing search (**Figure 4.1**).

Using simulated sequences as well as sequences from the 1000 Genomes Project, we compare the characteristics and performance the representative panel to the most diverse panel and randomly selected panels so that we can provide guidelines for investigators to use when planning sequencing studies with existing genotype data.

4.2 Materials and methods

4.2.1 Define the representative panel

4.2.1.1 Haploid case

Assume a sample of 2*n* haplotypes, we want to choose 2*k* haplotypes as a reference panel ($k \leq n$). We represent the selected 2*k* references in R as $I_1, I_2, \ldots, I_{2k}$ and represent the unselected 2*n* - *2k* haplotypes in U as J_1, J_2, ..., $J_{2n\text{-}2k}$. For each haplotype $j \in$ U, we represent the minimum distance to the haplotypes in R as $d_j = \min_{i \in \mathrm{R}} \{D_{ji}\}$, where *i* is the haplotype in R that is the closest to *j* and D_{ji} represents the pair-wise Hamming distance between haplotypes $j \in$ U and $i \in$ R.

The sum of minimum distance for one realization of R and U, represented by (R, U) is,

$$(\mathrm{R}, \mathrm{U}) = \sum_{\mathrm{j} \in \mathrm{U}} \mathrm{d_j} = \sum_{\mathrm{j} \in \mathrm{U}} \min_{\mathrm{i} \in \mathrm{R}} \{\mathrm{D_{ji}}\}.$$

Our goal is to find the realization with minimum distance among all possible realizations of (R, U) with size R_{2k} and $\mathrm{U}_{2n\text{-}2k}$, the "minimum of minimums", represented by $(\hat{\mathrm{R}}, \hat{\mathrm{U}})$,

$$\left(\hat{\mathrm{R}}, \hat{\mathrm{U}}\right) = \arg\{(\mathrm{R}, \mathrm{U})\} = \arg\min(\sum_{\mathrm{j} \in \mathrm{U}} \min_{\mathrm{i} \in \mathrm{R}} \{\mathrm{D_{ji}}\}).$$

4.2.1.2 Diploid case

Assume a sample of 2n haplotypes, which we randomly pair two haplotypes without replacement and form into n diploid individuals. We want to choose k diploid individuals out of n phased diploid individuals ($k \leq n$). We represent the selected k diploid individuals in R as (I_{1a}, I_{1b}), (I_{2a}, I_{2b}), ..., (I_{ka}, I_{kb}) and represent the unselected n - k individuals in U as (J_{1a}, J_{1b}), (J_{2a}, J_{2b}), …, ($J_{(n-k)a}$, $J_{(n-k)b}$), where all the individuals are phased and they are in arbitrary order.

For each individual j ϵ U, the minimum distance to the selected subset is haplotype i ϵ R, defined as

$$d_j = min_{i\epsilon \mathrm{R,s\epsilon(a,b)}} D_{j_a i_s} + min_{i\epsilon \mathrm{R,s\epsilon(a,b)}} D_{j_b i_s}..$$

$D_{j_s i_t}$ represents the pair-wise Hamming distance between haplotype j_s and i_t for s, t ϵ (a, b).

Our goal is to find the realization with minimum distance out of all the possible realizations with size R_k and U_{n-k}, represented by $(\hat{\mathrm{R}}, \hat{\mathrm{U}})$,

$$(\hat{\mathrm{R}}, \hat{\mathrm{U}}) = \arg\min(\sum_{\mathrm{j\in U}} \mathrm{d_j})$$

$$= \arg\min\{\textstyle\sum_{\mathrm{j\in U}}(min_{i\epsilon \mathrm{R,s\epsilon(a,b)}} D_{j_a i_s} + min_{i\epsilon \mathrm{R,s\epsilon(a,b)}} D_{j_b i_s})\}.$$

4.2.2 Hill-climbing search algorithm

Hill-climbing is a greedy local search algorithm that results in a local optimum. To increase the chance of reaching the global minimum and to speed up the search, we randomly divide the study sample into R and U with a certain size for 100 times and start the hill-climbing search with set of (R, U) that has the smallest distances (**Figure 4.1**).

4.2.2.1 Implementation: haplotype case

1. Randomly select 100 subsets (R_0, size 2*k* haplotypes), calculate the distances of (R_0,U_0) for each selection.
2. Select the set of (R_0,U_0) that has the smallest distance as starting (R, U).
3. Randomly replace one haplotype in R with one haplotype from U, recalculate (R, U)', if (R,U)'> (R,U), accept the replacement, otherwise keep the previous subset selection.
4. Repeat step 3 for 100,000 times, record the final selection of (R, U).

4.2.2.2 Implementation: diploid case

1. Randomly pair two haplotypes into diploid without replacement.
2. Randomly select 100 subsets (R_0, size *k* diploids), calculate the distances of (R_0,U_0) for each selection.
3. Select the set of (R_0,U_0) that has the smallest distance as the starting (R, U).
4. Randomly replace one pair of haplotypes in R with one pair of haplotypes from U, recalculate (R, U)'. If (R,U)'> (R,U), accept the replacement, otherwise keep the previous subset selection.
5. Repeat step 4 for 100,000 times, record the final selection of (R, U).

4.2.3 Diverse reference panel

The most diverse panel and diverse diploid are the same as described in Chapter 3, which are obtained from the greedy algorithm.

4.2.4 Imputation accuracy

We employ *minimac* (Howie et al. 2012) as one of the best-performing methods, which is an extension of MaCH (Li et al. 2010) for phased diploid data. To evaluate the imputation accuracy of imputed sites across all individuals in imputed datasets. For each site *j*, the concordance rate for the minor allele is

$$X_j = \{1 - \frac{\sum_{i=1}^{n} |g_{ij} - \hat{g}_{ij}|}{\sum_{\mathrm{i}=1}^{\mathrm{n}} g_{ij}} : g_{ij} \in (1,2)\}.$$

g_{ij} and $\hat{g}_{ij}$ are the simulated genotype and imputed genotype for individual *i* at site *j*, represented by the number of minor alleles in that individual (0, 1 and 2) at that site. *n* is the number of diploid individuals in the study sample.

Similarly, the concordance rate for the major allele of site *j* is

$$Y_j = 1 - \frac{\sum_{i=1}^{n} |g_{ij} - \hat{g}_{ij}|}{\sum_{\mathrm{i}=1}^{\mathrm{n}} (2 - g_{ij})} : g_{ij} \in (0,1)\}.$$

We compute the expected heterozygote concordance rate for site *j* by

$$H_j = 1 - [X_j(1 - Y_j) + Y_j(1 - X_j)].$$

X_j and Y_j are the allele concordance rate for the minor allele and the major allele, respectively.

4.2.5 Simulations

We simulate sequence data using the program *ms* (Hudson 2002) with parameters and datasets created the same as described in Chapter 3. Briefly we first remove singletons from the simulated sequences. We create the study samples by randomly choosing ~300 genotyped SNPs per Mb among markers with MAF ≥ 0.1 and mask the genotypes of all other sites. These masked sites are the markers in the study sample for imputation. We form diploid individuals by randomly pairing two haplotypes without replacement. We consider phased individuals, as we do not focus on phasing.

We simulated 50 datasets. In order to create datasets with imputation target region of 100 kb, 500 kb, 1 Mb, and 2 Mb, each with a flanking 450 kb region, we simulate 2000 haplotypes each with 2.9 Mb in total length for each dataset then create each datasets with variable lengths (**Figure 4.2**). We also vary reference sizes from 100, 200, 300, and 400 and vary genotyped marker density from 100, 300, 500, 700, to 900 SNPs per Mb. For each created dataset, we select a representative panel using our method for the haploid case and a representative panel for diploid case. For comparison, we also select the most diverse, the diverse diploid, and a randomly selected panel. We perform imputation with each selected panel and compare their performance.

4.2.6 The 1000 Genomes Project data

We apply our method to sequence data from the 1000 Genomes Project. We use the same phased data of 381 diploid individuals (762 haplotypes) from five closely related European populations described in Chapter 3. We remove singletons from the sample, selecting ten 1-Mb regions that are approximately evenly distributed across chromosome 20. We create study samples following similar procedures as the simulated data by selecting 300 SNPs per Mb for variants with MAF ≥ 0.1 and mask the genotypes for all other SNPs. For each region, we select 160 haplotypes from a total of 762 haplotypes as a reference panel. For each dataset, we impute with different reference types and compare the SNP discovery rates, allele concordance rates and expected heterozygote concordance rates.

4.3 Results

4.3.1 Number of iterations for the hill-climbing algorithm

To evaluate if the local optimum is a reasonable approximation to the global optimum, we repeat the search by random start multiple times and select the best one. For selecting 200 haplotypes out of a total 2000 haplotypes, we randomly start the hill-climbing search multiple times and record the distances (R,U) at different number of iterations. We find that the (R, U) distance drops quickly during the first 5000 iterations, then it slows down. Here in our simulation, we run the update until distance (R, U) reaches zero or up to a maximum of 100,000 iterations.

4.3.2 SNP discovery rate

For the 50 simulated datasets of each 2000 haplotypes, the number of imputed sites ranges from 5,104 to 5,909, with a mean number of 5,437 sites in a 1 Mb region. We compute the SNP discovery rate in each selected subset and imputed dataset for the 50 datasets. We consider a SNP as being discovered if at least one minor allele is present in the selected subset or the imputed dataset.

For variants with MAF ≤ 0.005, the representative subset has the highest SNP discovery rate in all cases, except that the most diverse subset has the highest discovery rate at subset size of 100. For variants with 0.005 < MAF ≤ 0.05, the representative subset has the highest SNP discovery rate, followed by the representative diploid, the diverse, the diverse diploid, and the random panel across different subset sizes. The randomly selected subset has the lowest SNP discovery rate across panel sizes compared to other types of subsets. The SNP discovery rates increase with the increase of MAFs and with the increase of subset sizes. For variants with 0.005 < MAF ≤ 0.05 and size of 400 haplotypes, the SNP discovery rate is close to 1 and the differences among different types of subsets are smaller (mean rate from 0.962 to 0.989) (**Figure 4.3**).

We observe the same pattern for SNP discovery rates in imputed datasets. The representative subset has the highest SNP discovery rate in all cases except at subset size of 100 and variants with MAF ≤ 0.005 (**Figure 4.3**).

4.3.3 Imputation accuracy

4.3.3.1 $\hat{r}^2$ from imputation outputs

As a measure of predicted imputation accuracy generated by MaCH, we compare the average $\hat{r}^2$ (defined in Chapter 3) for imputations with different reference types. **Figure 4.4** shows that $\hat{r}^2$ increases with increasing number of reference haplotypes. The representative panel performs the best in most cases, whereas the diverse panel works better only in imputing variants with MAF ≤ 0.005 using a reference panel size of 100 haplotypes.

4.3.3.2 Allele concordance rate

We next compare the minor allele concordance rate for imputations with different reference types. We observe a higher concordance rate with the increase of MAF or the increase of reference panel size. For variants MAF ≥ 0.005, the representative panel provides the best minor allele concordance rate, followed by the diploid representative, the diverse, the diploid diverse, and the randomly selected panel. The same order applies to variants with MAF < 0.005 except imputations with reference panel of 100 haplotypes (**Figure 4.5**).

4.3.3.3 Expected heterozygote concordance rate

The expected heterozygote concordance rate has exactly the same pattern as the allele concordance rate, and the individual values are also similar (**Figure 4.6**). We expect it is because the allele concordance rate for the major allele of each site is close to 1, thus, the expected heterozygote concordance rate for a site $H_j \approx 1 - [X_j(1\text{-}1)+1(1\text{-}X_j)] = X_j$, where X_j is the allele concordance rate for the minor allele of the site.

4.3.4 Different imputation lengths

To test the performances of different types of reference panels when impute regions of different lengths, we perform imputations of different lengths from 100 kb, 500 kb, 1 Mb, to 2 Mb by fixing the reference panel size at 200 and the maker density at 300 SNP per Mb. The performances of the proposed panels for imputation length of 500 kb or longer follows the order of the representative, the representative diploid, the diverse, the diverse diploid, and the random panel when comparing SNP discovery rate (**Figure 4.7**), $\hat{r}^2$ (**Figure 4.8**), minor allele concordance rate (**Figure 4.9**), and the expected concordance rate (**Figure 4.10**). But for imputation with 100 kb, the representative diploid performs the worst of all reference types.

4.3.5 Different marker densities in the study sample

We test how the maker density of 100, 300, 500, 700, and 900 SNPs per Mb affect imputations with each reference type. The SNP discovery rate (**Figure 4.11**), mean $\hat{r}^2$ (**Figure 4.12**), and minor concordance rate (**Figure 4.13**) and the expected concordance rate (**Figure 4.14**) slightly increase with increasing number of markers in the study sample. For variants with MAF ≥ 0.005, the representative panel provides the best performance, followed by the diploid representative, the diverse, the diploid diverse, and the randomly selected panel, whereas for rare variants with MAF < 0.005, the diverse panel provides a better performance than the representative diploid panel.

4.3.6 The 1000 Genomes data

For the 1000 Genomes data, we selected ten 1-Mb regions that are evenly distributed across chromosome 20. The number of imputed sites ranges from 2,769 to 4,606, with mean equal to 3,873 sites within a 1 Mb region.

The imputation accuracy for imputations from the 1000 Genomes data is lower than that from the simulated data. The proposed panels all have better performance than the randomly selected reference panels. When comparing the SNP discovery (**Figure 4.15**), $\hat{r}^2$ (**Figure 4.16**), the minor allele concordance rate (**Figure 4.17**) and the expected heterozygote concordance rate (**Figure 4.18**), the diverse panel provides the best performance among all reference types. The representative panel and representative diploid panel perform in between the diverse and the diverse diploid for variants with

MAF ≥ 0.005. For rare variants with MAF < 0.005, the diploid diverse performs better than the representative and the representative diploid.

4.4 Discussion

In this chapter, we propose the representative sample for planning sequencing studies. Using simulated sequences, the representative panel performs better than the diverse and the randomly selected reference panel in recovering more polymorphic sites from the study sample and in providing higher imputation accuracy under most of our simulation settings, whereas the diverse reference panel provides better or comparable performance to the representative panel when imputing rare variants (MAF ≤ 0.005) or with a small reference size (e.g. 100 haplotypes) in simulated data with study individuals from one population. In the 1000 Genomes data with study individuals from closely related European populations, the most diverse panel works better than other types of reference panels.

We expect our method to be applicable to a target genomic region for individuals from one population or from closely related populations. For our test regions from 100 kb up to 2 Mb in the simulated data, the representative panel provides better performance with increasing imputation lengths. This might be because the representative algorithm is based on the similarity between haplotypes, and longer haplotypes provide more information. For the diverse panel, the lengths of imputation regions slightly affect the performance of the diverse panel with the best results achieved at the 500 kb region, indicating there might be an optimal length where the constructed tree approximates the ancestral relatedness the best for the most diverse panel to work.

To evaluate the performance of the selected panels in genotype imputation, we find that the measures of the minor allele concordance rate and the expected heterozygote concordance rate provide similar results for imputation accuracy. We also find that a higher SNP discovery rate will often result in a better imputation $\hat{r}^2$ and a higher allele concordance rate in imputations.

One limitation for the implementation of the most representative panel is that our hill-climbing based search can only obtain a local minimum, which might be very different from the global minimum. This might count partly why the diverse panel provides a better performance than the representative panel when imputing data from the 1000 Genomes Project. In our simulation, we select multiple (R, U)s but only select the one that has the smallest distance as the starting point for the hill-climbing search limited by the number of datasets in the simulation. To further optimize the algorithm in practice, we can randomly pick multiple starting points, perform the hill-climbing search for each starting point, and select the one that provides the smallest final (R, U) distance to increase the chance to reach the global minimum.

In summary, we present the most representative sampling strategy for planning sequence studies. Using simulated sequence data and real sequence data from the 1000 Genomes Project, we show the most representative panel performs better than the most diverse panel and randomly selected panels in the majority of simulation settings for individuals from one population, while the most diverse panel provide the best performance when imputing sequences for individuals from closely related populations in the 1000 Genomes data. Further characterizing these two proposed strategies will certainly provide more information for investigators to choose when planning sequencing studies.

Figure 4.1 Illustration of using multiple random starts in the hill-climbing search. Shown is a one-dimensional state-space of all (R, U) distances. Because the hill-climbing search only moves in one direction, here is to decreasing distances, it is important where the search starts on the state space. To speed up the hill-climbing search and increase the chance to reach the global minimum, we initiate multiple random starts (dot with an arrow point to it) and select the one that has the smallest distance as the starting state (marked as bold arrow) for the hill-climbing update (Russell and Norviq 2009).

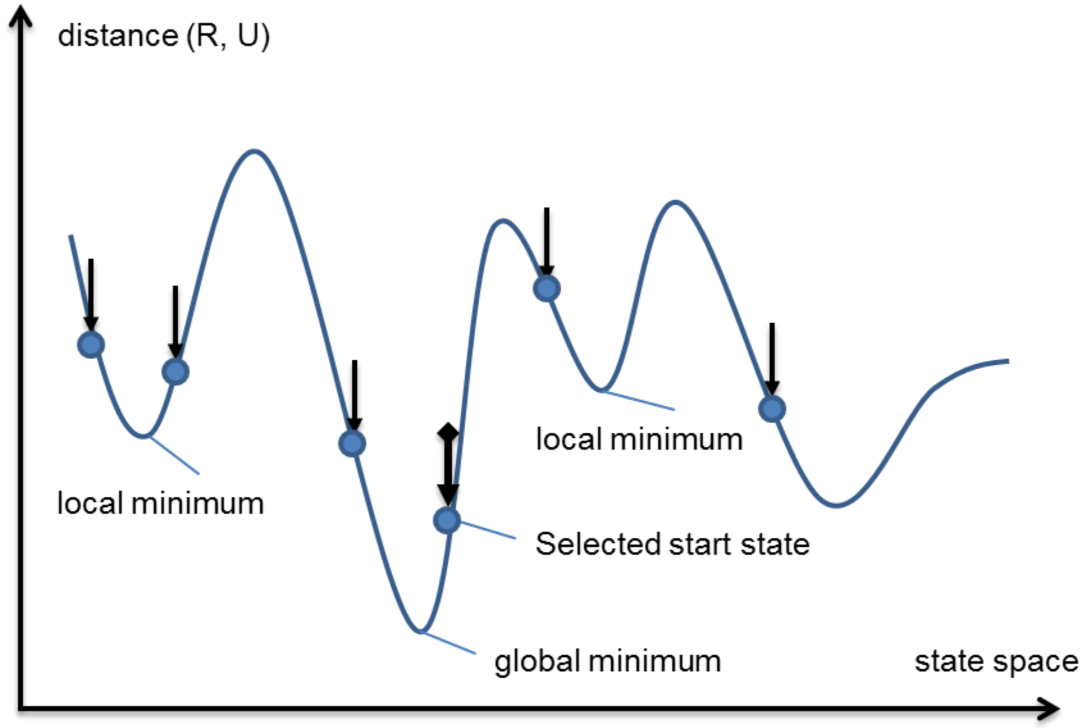

Figure 4.2 Sequence data simulation scheme. For a total of 2.9 Mb, we impute the middle region from 100 kb, 500 kb, 1 Mb, to 2 Mb, with 450 kb flanking region at both ends.

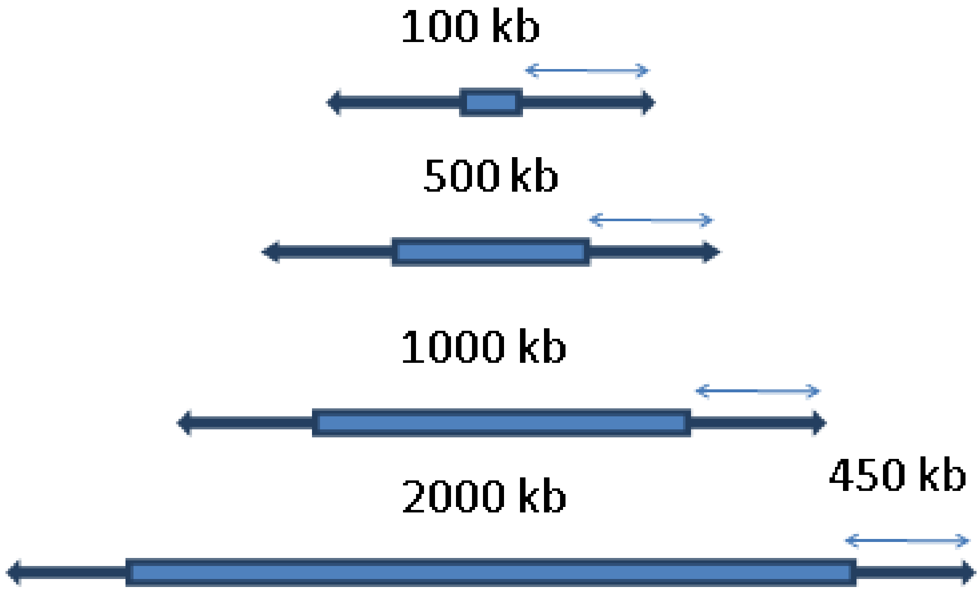

Figure 4.3 SNP discovery rate in selected subsets and imputed datasets. A and B: SNP discovery rate in reference panels. C and D: SNP discovery rate in imputed datasets. The horizontal-axis is the reference panel sizes, The vertical-axis is the discovery rate SNP discovery rates in selected subset (A and B) and imputed datasets (C and D) for variants with MAF ≤ 0.05. Data are from 50 simulated datasets. Error bars are the standard errors at each reference panel size for each variant group. Imputation length is 1 Mb.

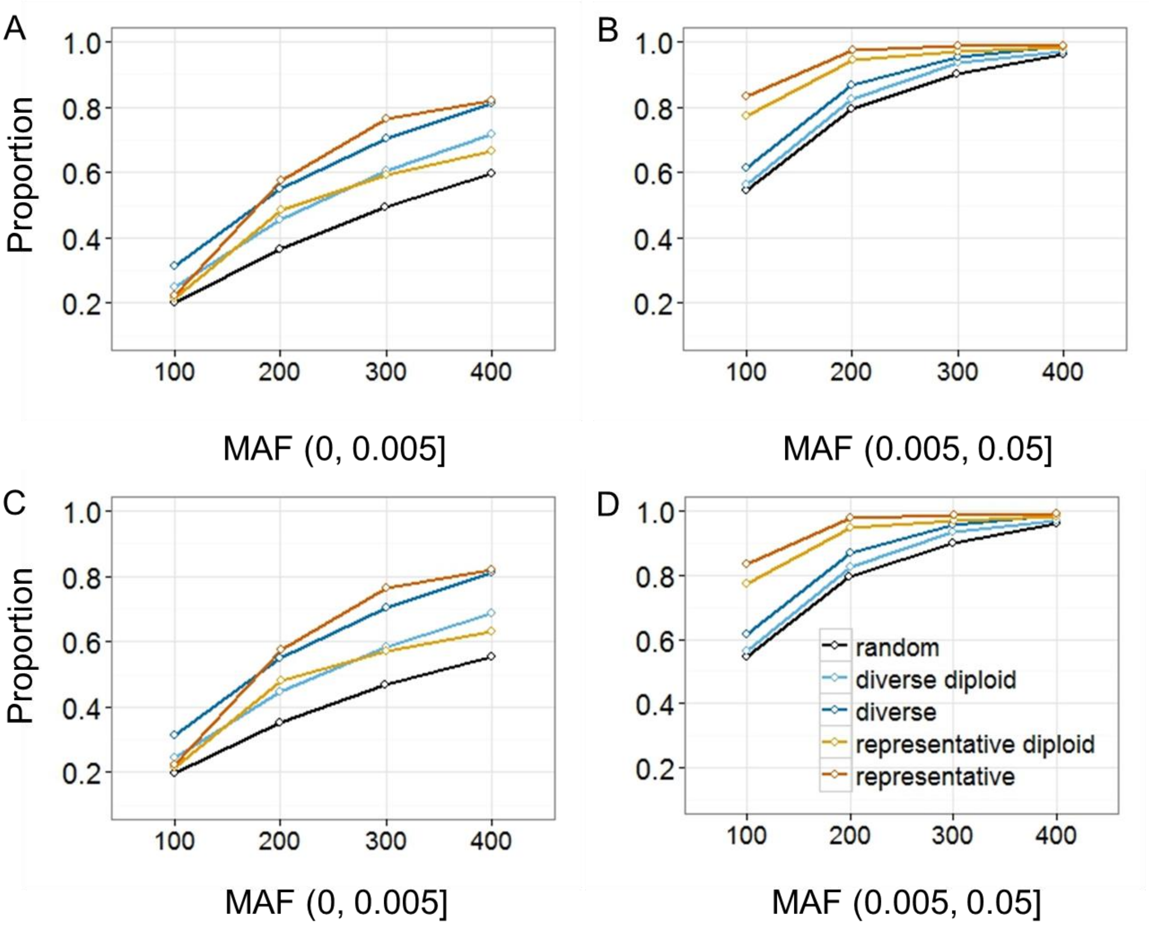

Figure 4.4 R-square for imputations with different reference panel sizes. Data are from 50 simulated datasets. Error bars are the standard errors at each reference panel size for each variant group. Imputation length is 1 Mb.

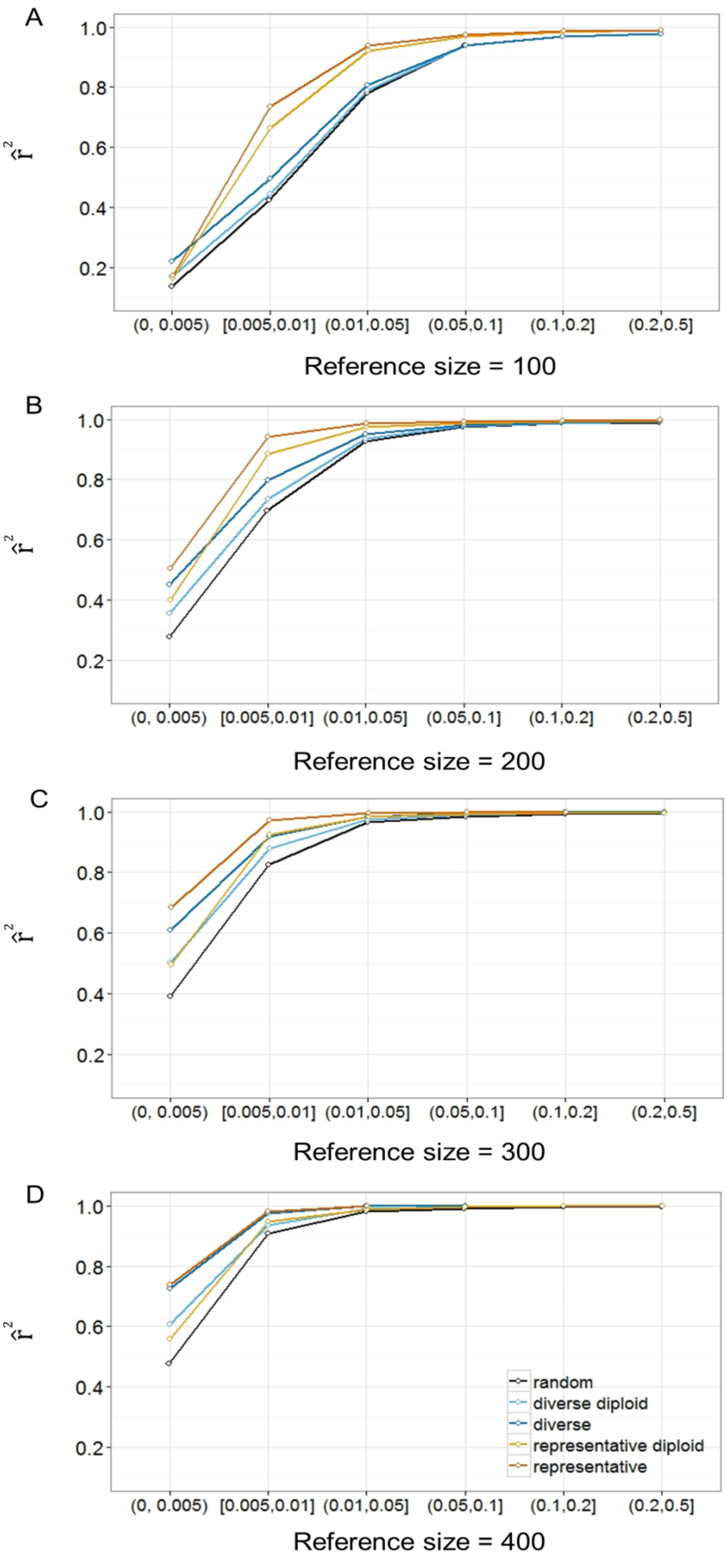
A
1.0
0.8
0.6
0.4
0.2
$\hat{r}^2$
(0, 0.005)
[0.005,0.01]
(0.01,0.05]
(0.05,0.1]
(0.1,0.2]
(0.2,0.5]
Reference size = 100
B
1.0
0.8
0.6
0.4
0.2
$\hat{r}^2$
(0, 0.005)
[0.005,0.01]
(0.01,0.05]
(0.05,0.1]
(0.1,0.2]
(0.2,0.5]
Reference size = 200
C
1.0
0.8
0.6
0.4
0.2
$\hat{r}^2$
(0, 0.005)
[0.005,0.01]
(0.01,0.05]
(0.05,0.1]
(0.1,0.2]
(0.2,0.5]
Reference size = 300
D
1.0
0.8
0.6
0.4
0.2
$\hat{r}^2$
random
diverse diploid
diverse
representative diploid
representative
(0, 0.005)
[0.005,0.01]
(0.01,0.05]
(0.05,0.1]
(0.1,0.2]
(0.2,0.5]
Reference size = 400

Figure 4.5 Allele concordance rate for imputations of 1 Mb with different reference panel types. Data are from 50 datasets. For each dataset, we performed one imputation with each reference panel. The error bars are the standard errors of concordance rates of imputed markers at each MAF group.

Legend: Reference types

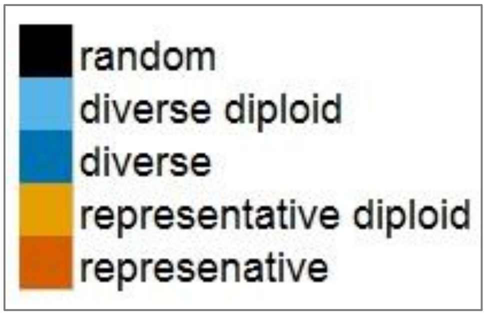

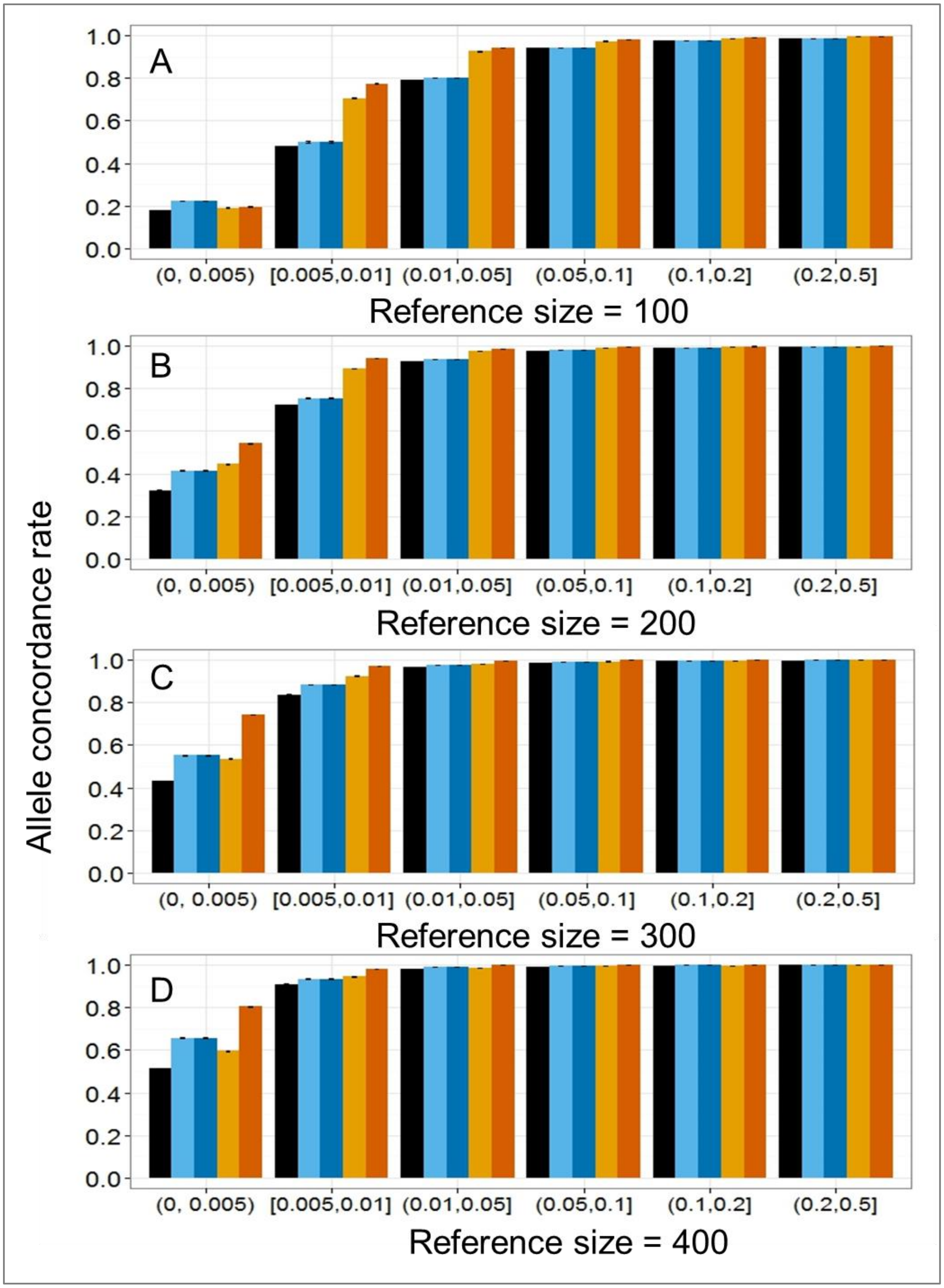
A
Reference size = 100
B
Reference size = 200
C
Reference size = 300
D
Reference size = 400
Allele concordance rate
0.0
0.2
0.4
0.6
0.8
1.0
(0, 0.005)
[0.005,0.01]
(0.01,0.05]
(0.05,0.1]
(0.1,0.2]
(0.2,0.5]

Figure 4.6 The Expected heterozygote concordance rate. Data are from 50 datasets. For each dataset, we performed one imputation with each reference panel. The error bars are the standard errors of concordance rates of imputed markers at each MAF group.

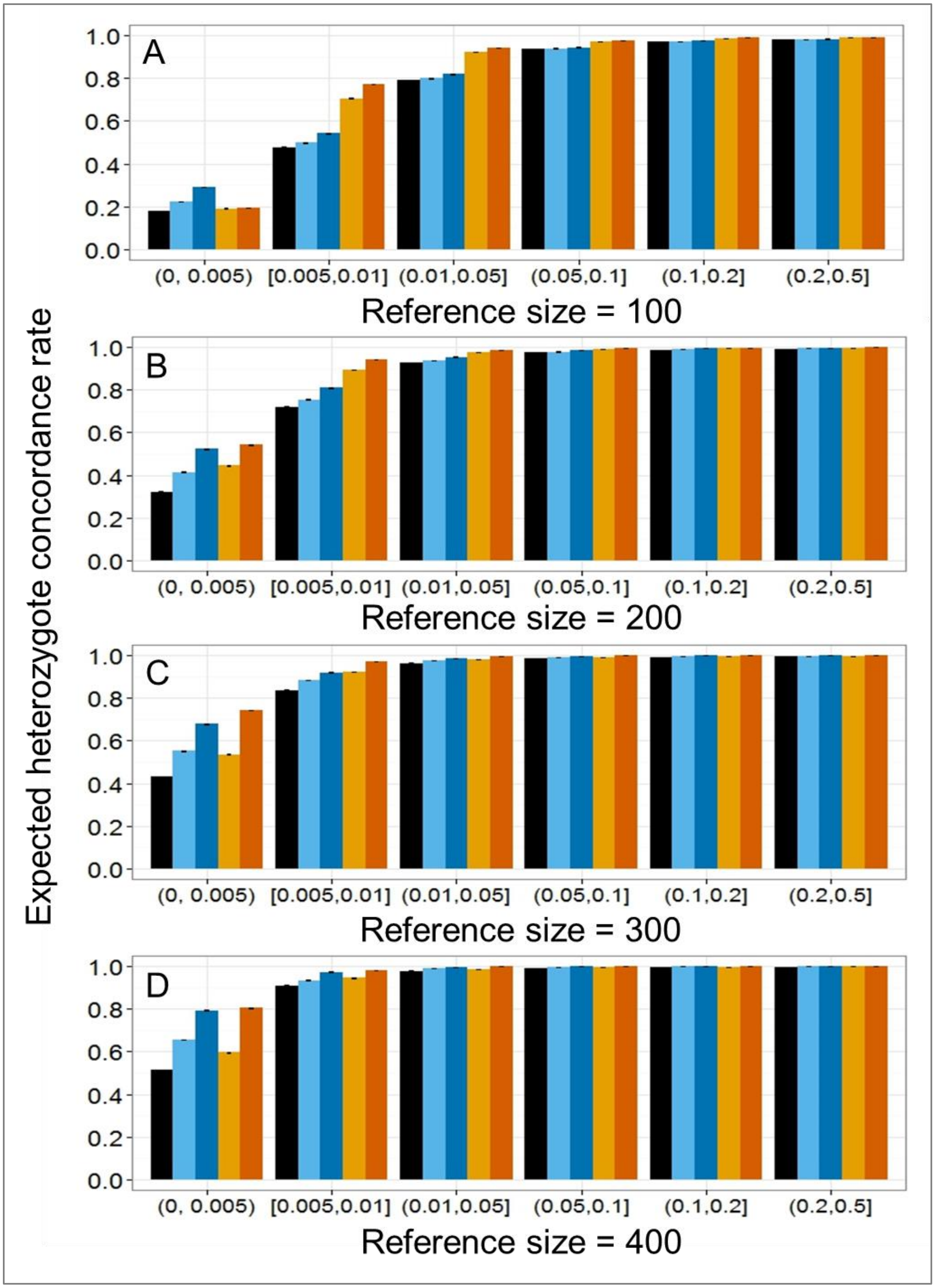
A
B
C
D
1.0
0.8
0.6
0.4
0.2
0.0
(0, 0.005)
[0.005,0.01]
(0.01,0.05]
(0.05,0.1]
(0.1,0.2]
(0.2,0.5]
Reference size = 100
Reference size = 200
Reference size = 300
Reference size = 400
Expected heterozygote concordance rate

Figure 4.7 SNP discovery rate for different imputation lengths. Data from 50 datasets for each imputation length. Maker density 300 SNPs per Mb. Reference panel size of 200 haplotypes.

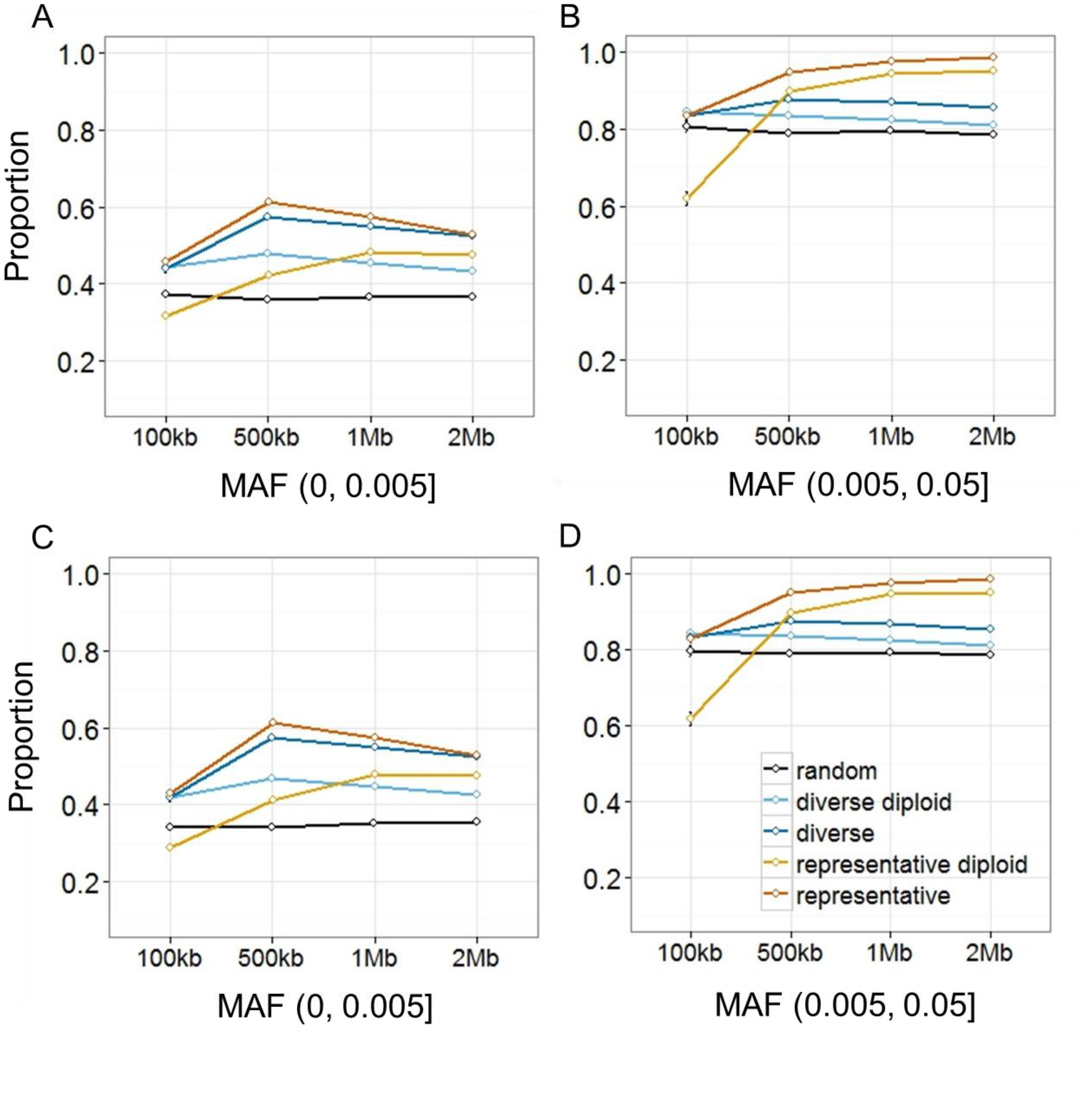

Figure 4.8 R-square for imputations with different target lengths. Data from 50 datasets for each imputation length. Maker density 300 SNPs per Mb. Reference panel size of 200 haplotypes.

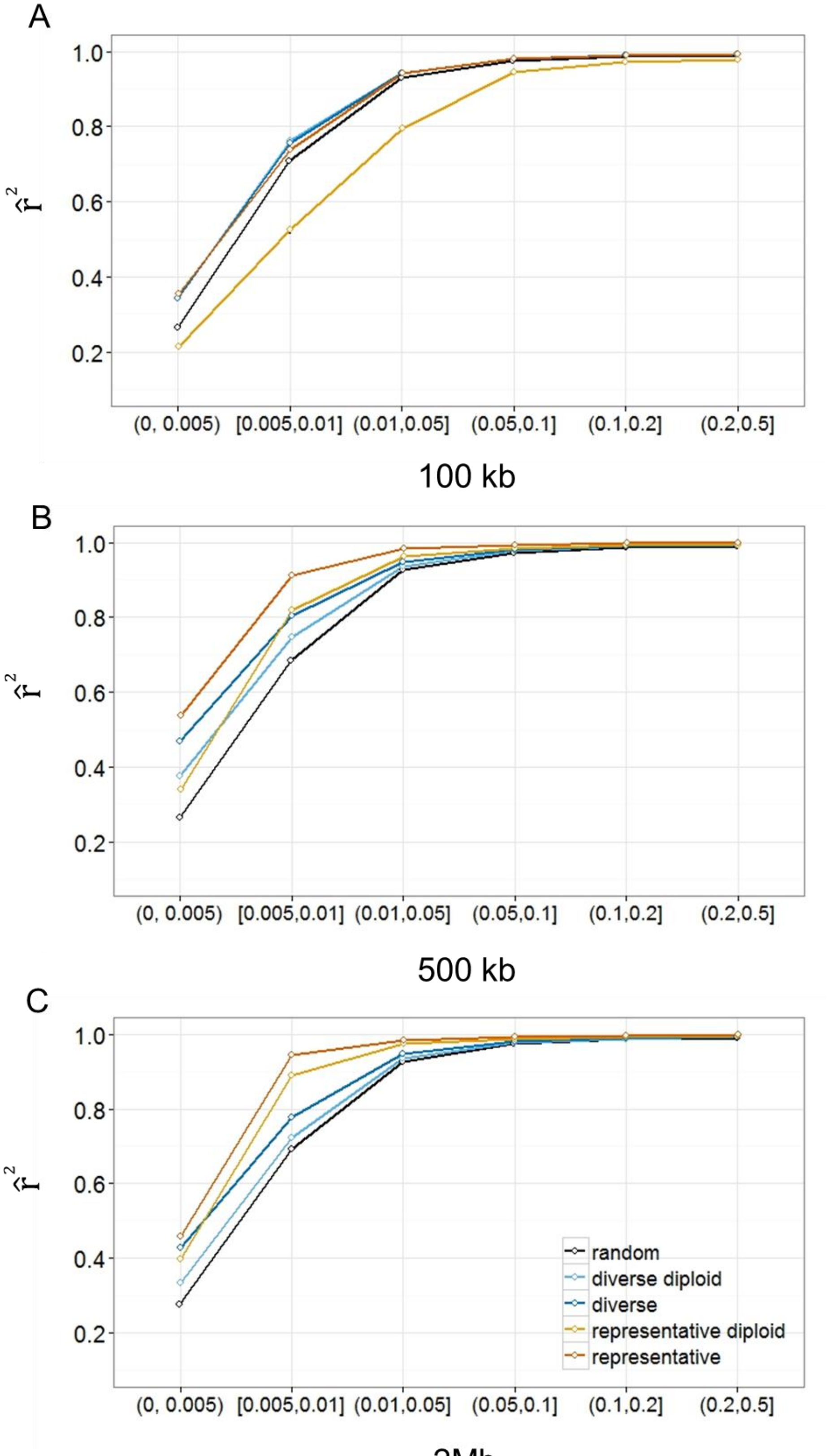

100 kb

500 kb

2Mb

Figure 4.9 Allele concordance rate with different imputation lengths. Data are from 50 datasets for each imputation length. Maker density 300 SNPs per Mb. Reference panel size of 200 haplotypes.

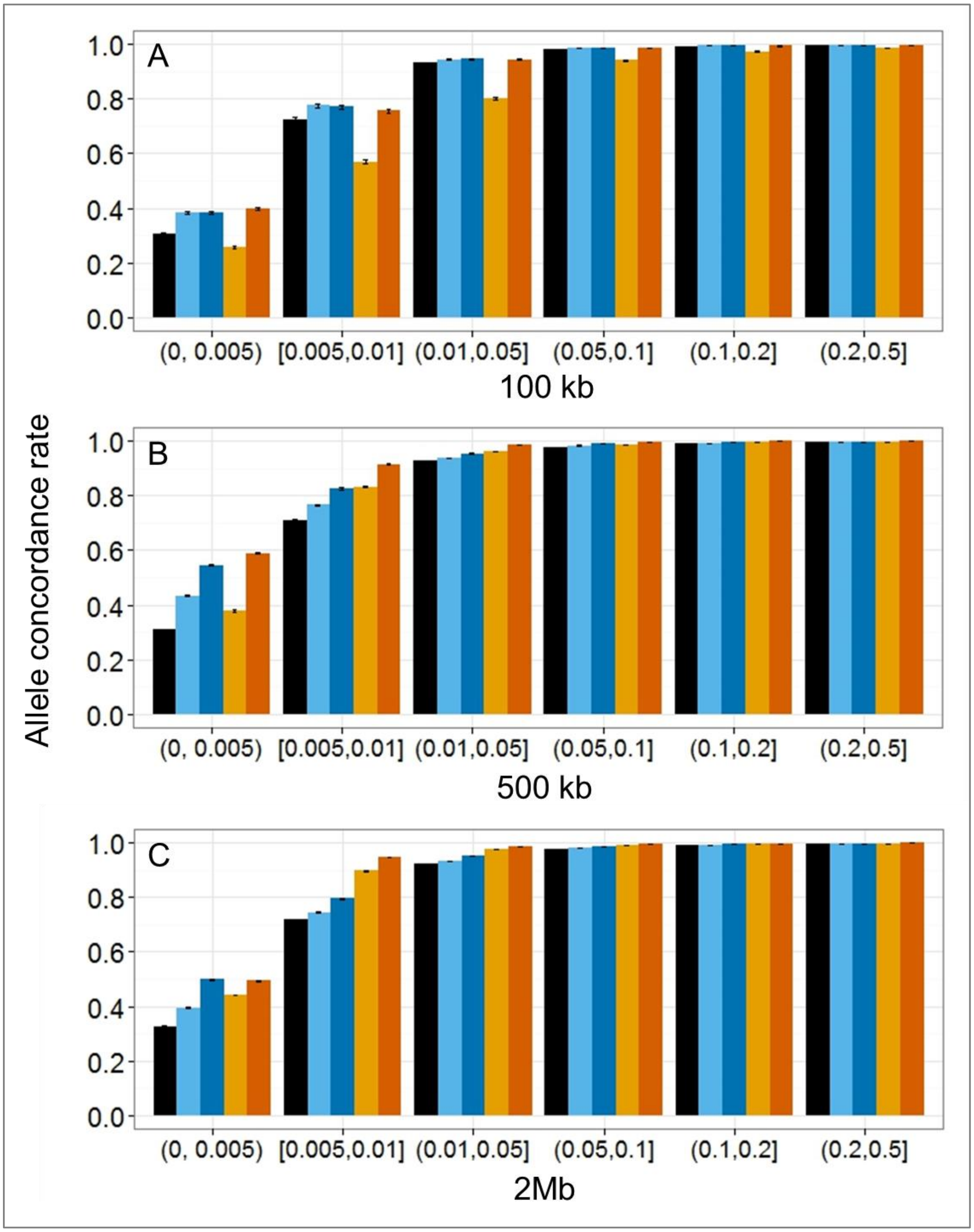

Figure 4.10 Expected heterozygote concordance rate for different imputation lengths. Data are from 50 datasets for each imputation length. Maker density 300 SNPs per Mb. Reference panel size of 200 haplotypes.

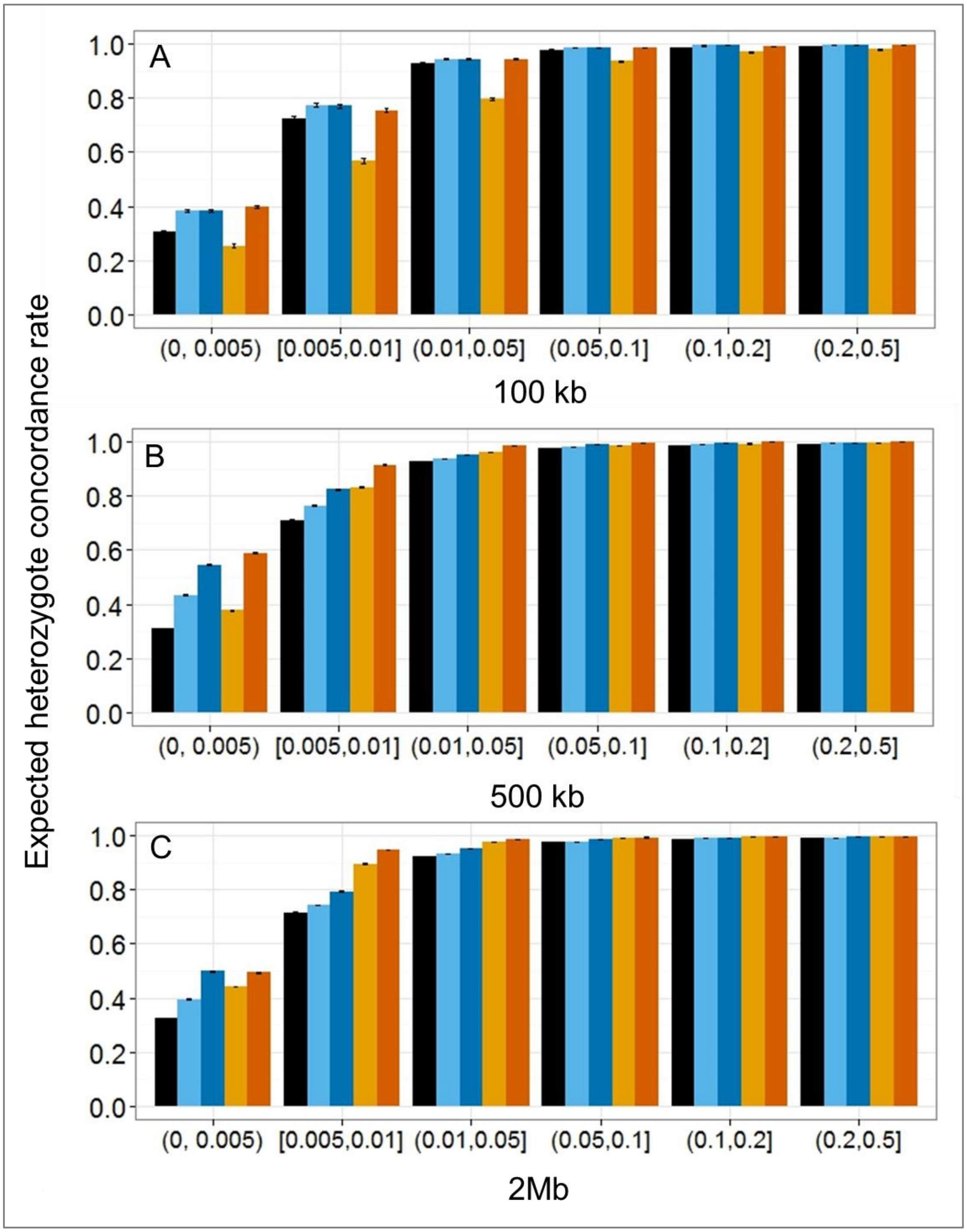

Figure 4.11 SNP discovery rate for imputations with different marker densities. Data are from 50 datasets for each maker density. Imputation length is 1Mb. Reference panel size of 200 haplotypes. Horizontal axis represents number of SNPs per Mb in the study sample. A and B are the discovery rates from selected reference panels. C and D are the discovery rate from imputed datasets.

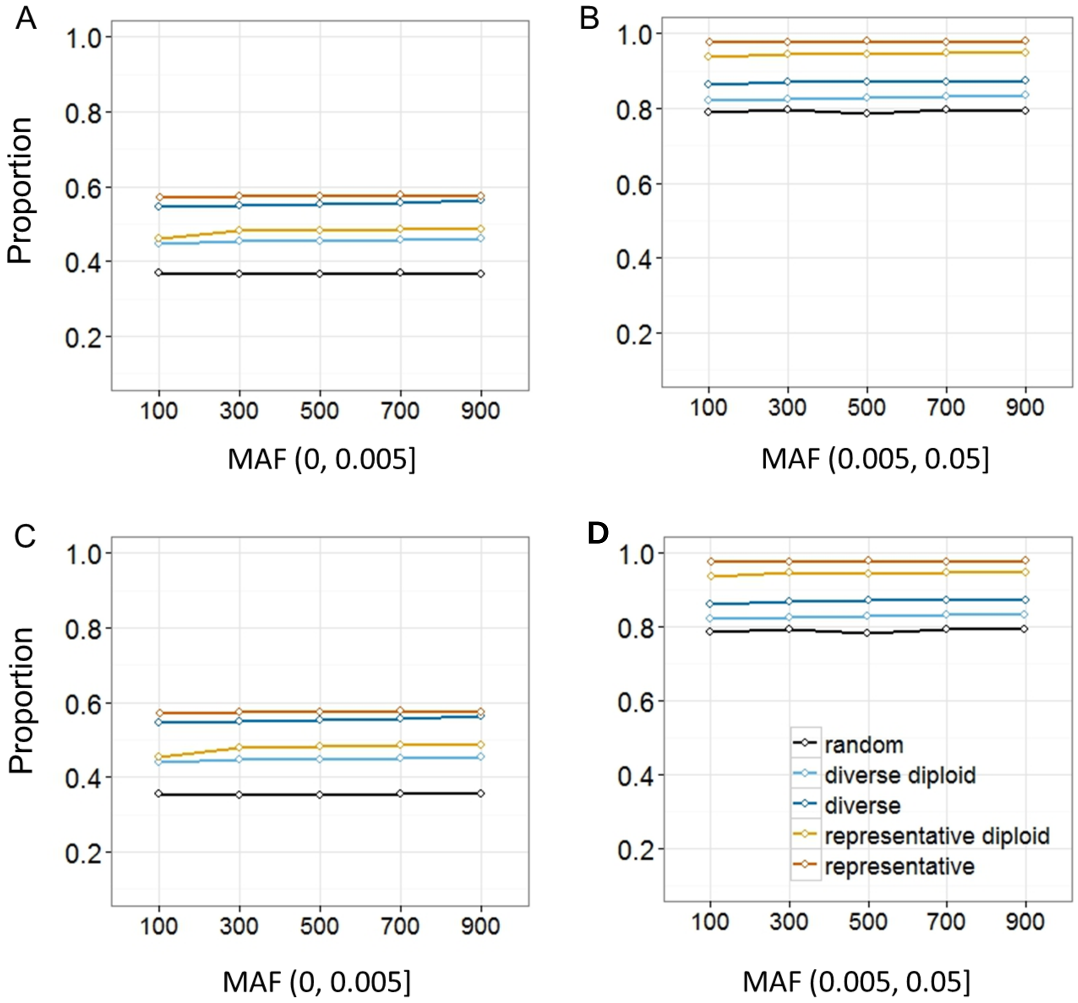

Figure 4.12 R-square for imputations with different marker densities. Data are from 50 datasets for each maker density. Imputation length is 1Mb. Reference panel size of 200 haplotypes. Horizontal axis represents number of SNPs per Mb in the study sample. A and B are the discovery rates from selected reference panels. C and D are the discovery rate from imputed datasets.

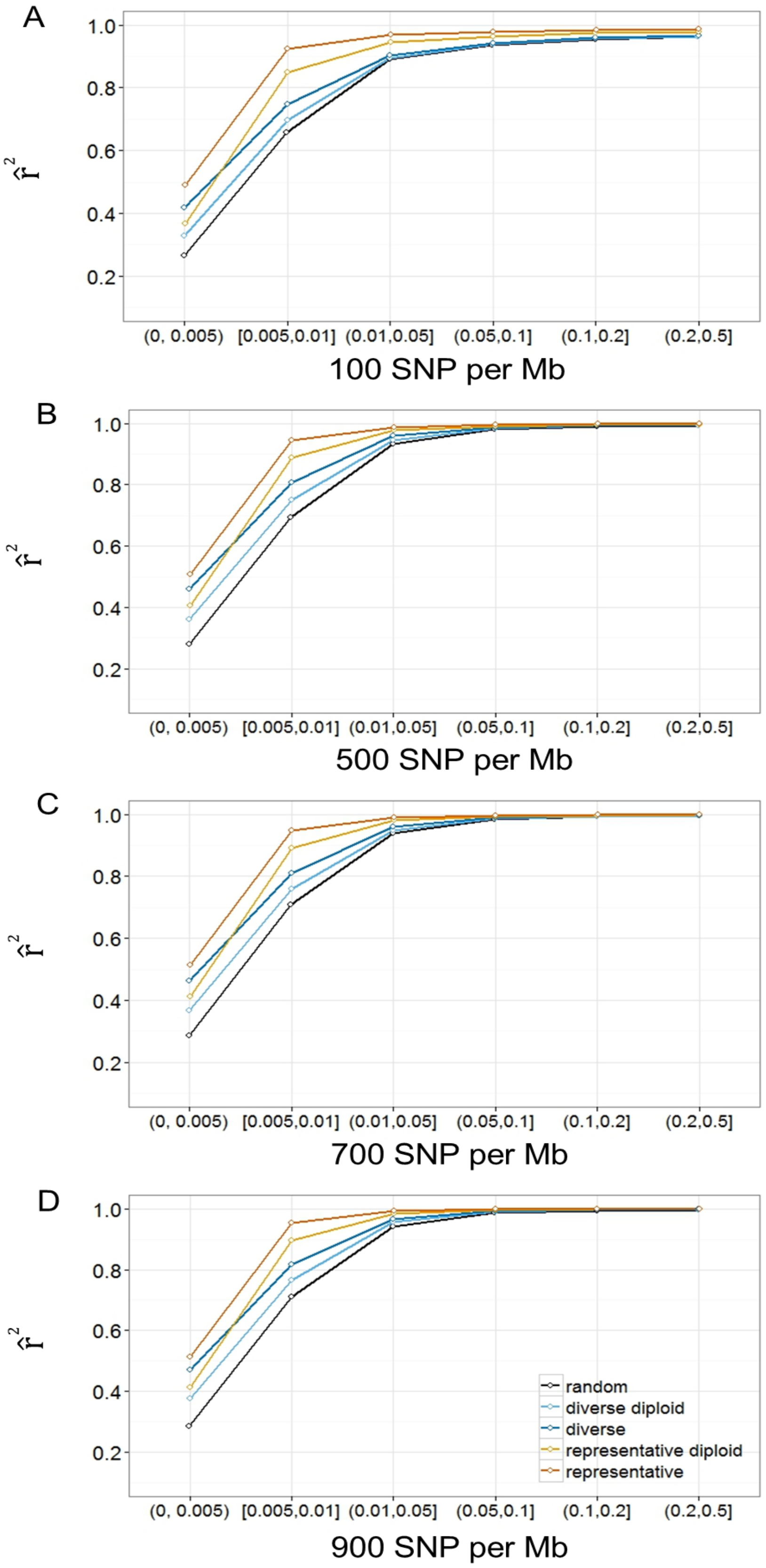
A
1.0
0.8
0.6
0.4
0.2
$\hat{r}^2$
(0, 0.005)
[0.005,0.01]
(0.01,0.05]
(0.05,0.1]
(0.1,0.2]
(0.2,0.5]
100 SNP per Mb
B
500 SNP per Mb
C
700 SNP per Mb
D
900 SNP per Mb
random
diverse diploid
diverse
representative diploid
representative

Figure 4.13 Allele concordance rate for imputations with different marker density in study samples. Data are from 50 datasets for each maker density. Imputation length is 1Mb. Reference panel size of 200 haplotypes. Horizontal axis represents number of SNPs per Mb in the study sample. A and B are the discovery rates from selected reference panels. C and D are the discovery rate from imputed datasets.

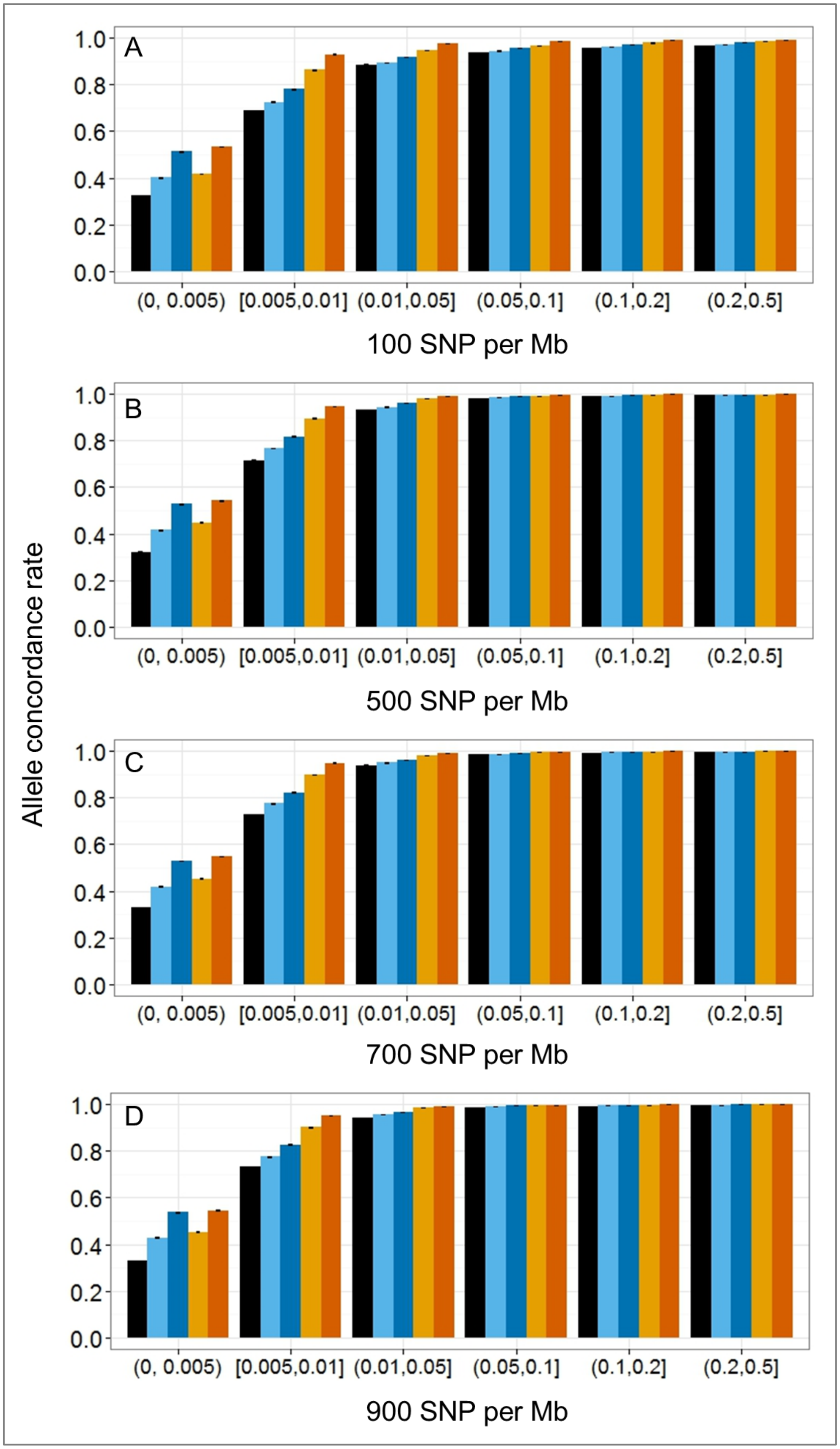
Allele concordance rate
A
1.0
0.8
0.6
0.4
0.2
0.0
(0, 0.005)
[0.005,0.01]
(0.01,0.05]
(0.05,0.1]
(0.1,0.2]
(0.2,0.5]
100 SNP per Mb
B
500 SNP per Mb
C
700 SNP per Mb
D
900 SNP per Mb

Figure 4.14 Expected heterozygote concordance rate for different maker density. Data are from 50 datasets for each maker density. Imputation length is 1Mb. Reference panel size of 200 haplotypes. Horizontal axis represents number of SNPs per Mb in the study sample. A and B are the discovery rates from selected reference panels. C and D are the discovery rate from imputed datasets.

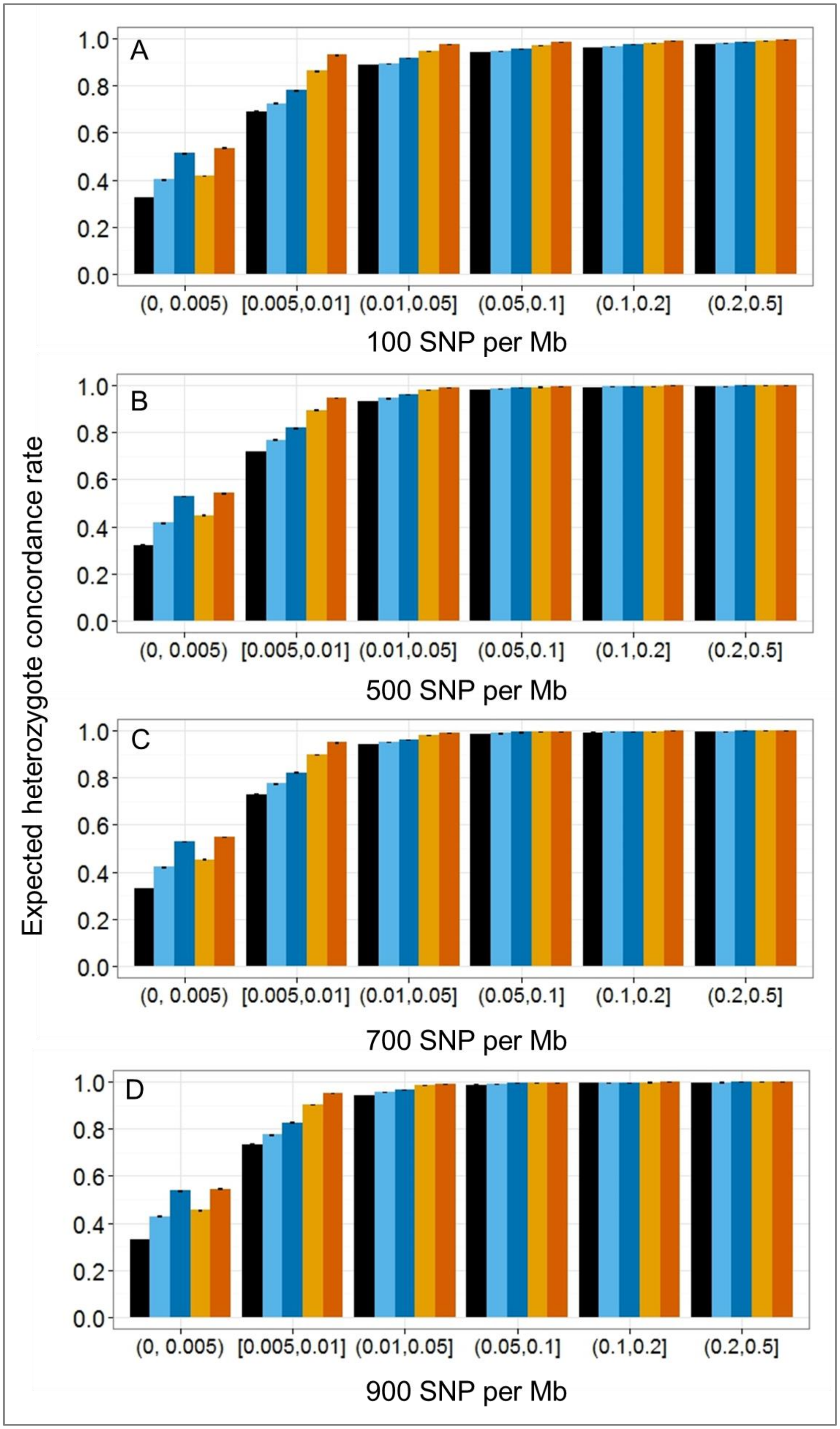
Expected heterozygote concordance rate
A
B
C
D
1.0
0.8
0.6
0.4
0.2
0.0
(0, 0.005)
[0.005,0.01]
(0.01,0.05]
(0.05,0.1]
(0.1,0.2]
(0.2,0.5]
100 SNP per Mb
500 SNP per Mb
700 SNP per Mb
900 SNP per Mb

Figure 4.15 SNP discovery rate for the 1000 Genomes data. Data are from ten regions of 1 Mb from chromosome 20 of EUR ancestry. For a total 381 diploid individuals, select 160 haplotypes as a reference panel. Horizontal axis is the MAF group.

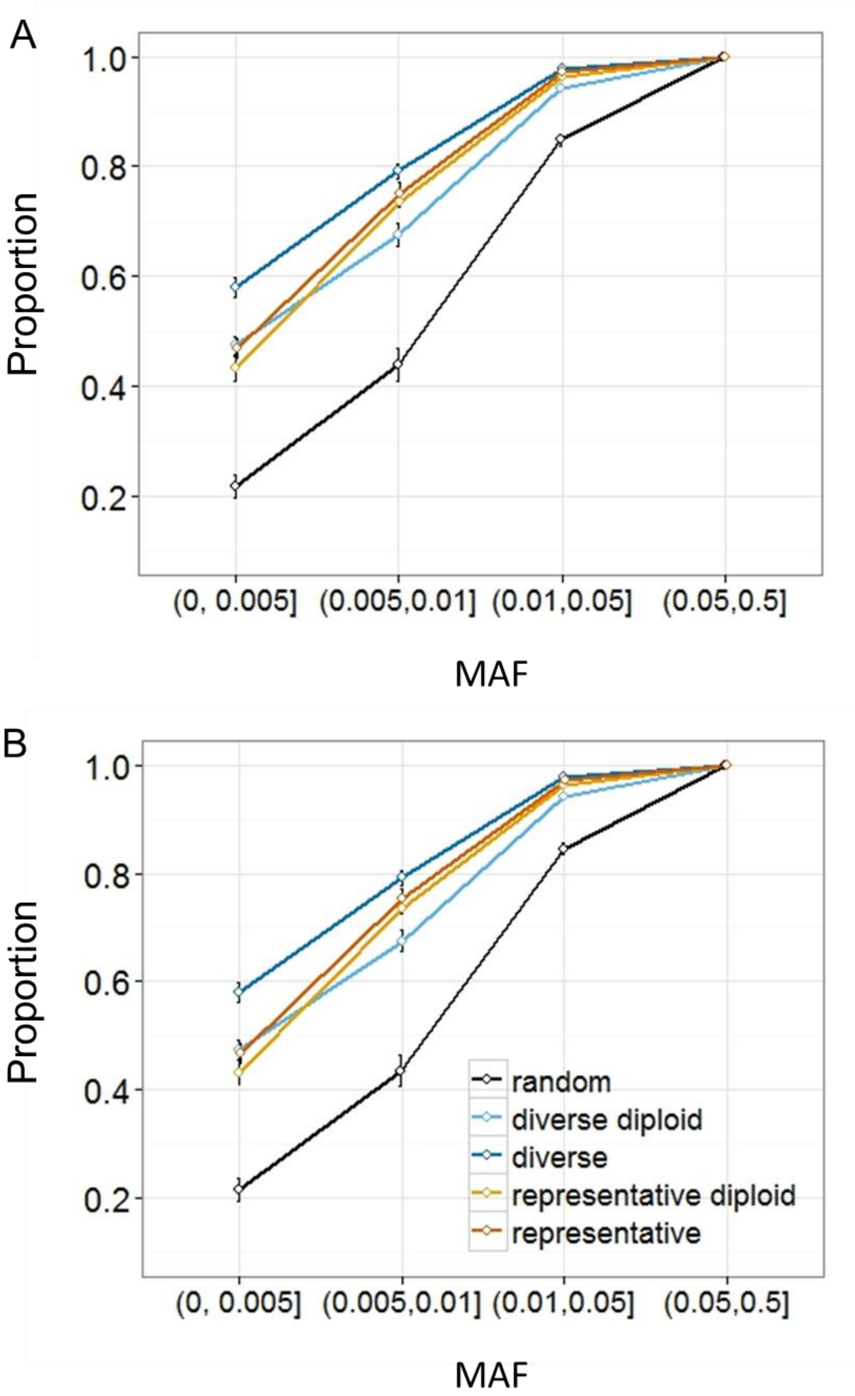

Figure 4.16 R-square for imputations of the 1000 Genomes data. Data are from ten regions of 1 Mb from chromosome 20 of EUR ancestry. For a total 381 diploid individuals, select 160 haplotypes as a reference panel. Horizontal axis is the MAF group.

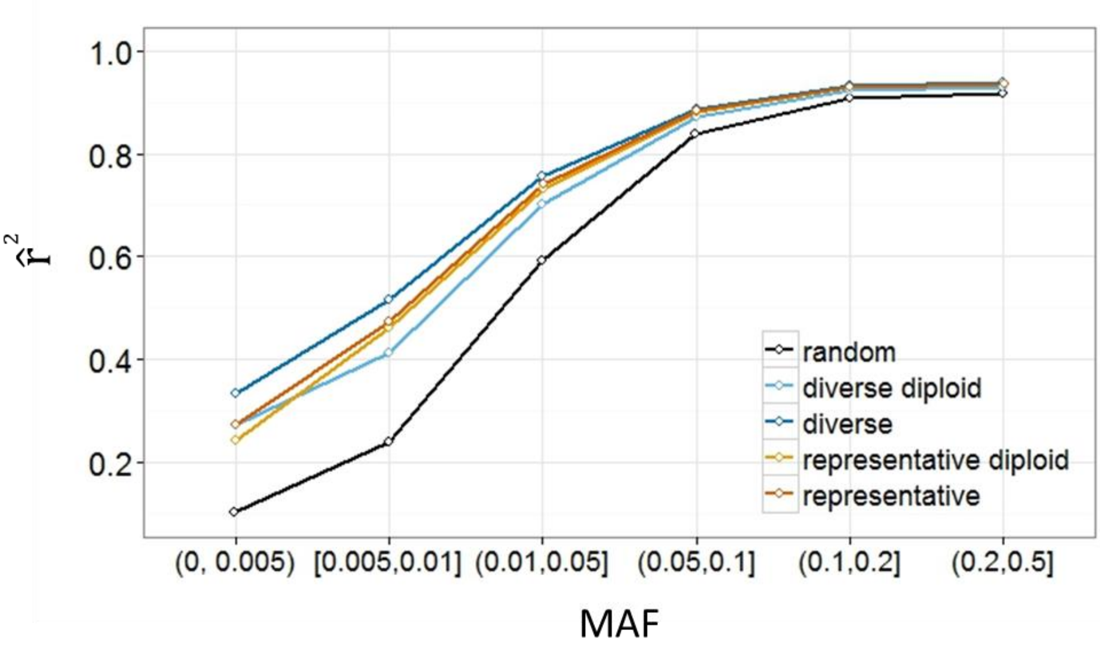

Figure 4.17 Allele concordance rate for the 1000 Genomes data. Data are from ten regions of 1 Mb from chromosome 20 of EUR ancestry. For a total 381 diploid individuals, select 160 haplotypes as a reference panel. Horizontal axis is the MAF group.

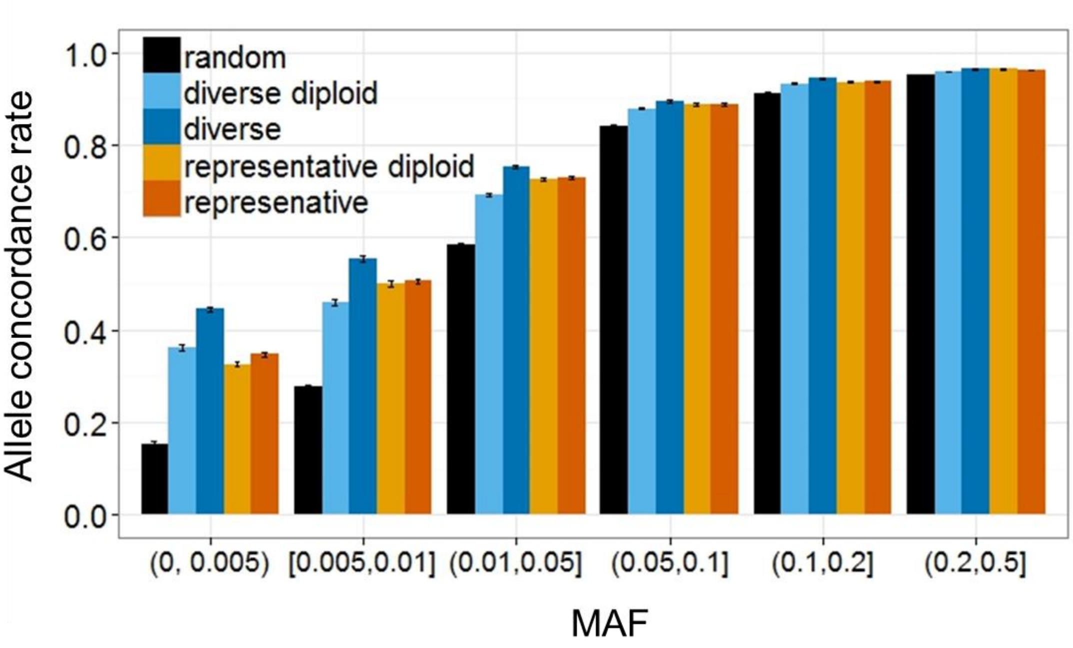

Figure 4.18 Expected heterozygote concordance rate for the 1000 Genomes data. Data are from ten regions of 1 Mb from chromosome 20 of EUR ancestry. For a total 381 diploid individuals, select 160 haplotypes as a reference panel. Horizontal axis is the MAF group.

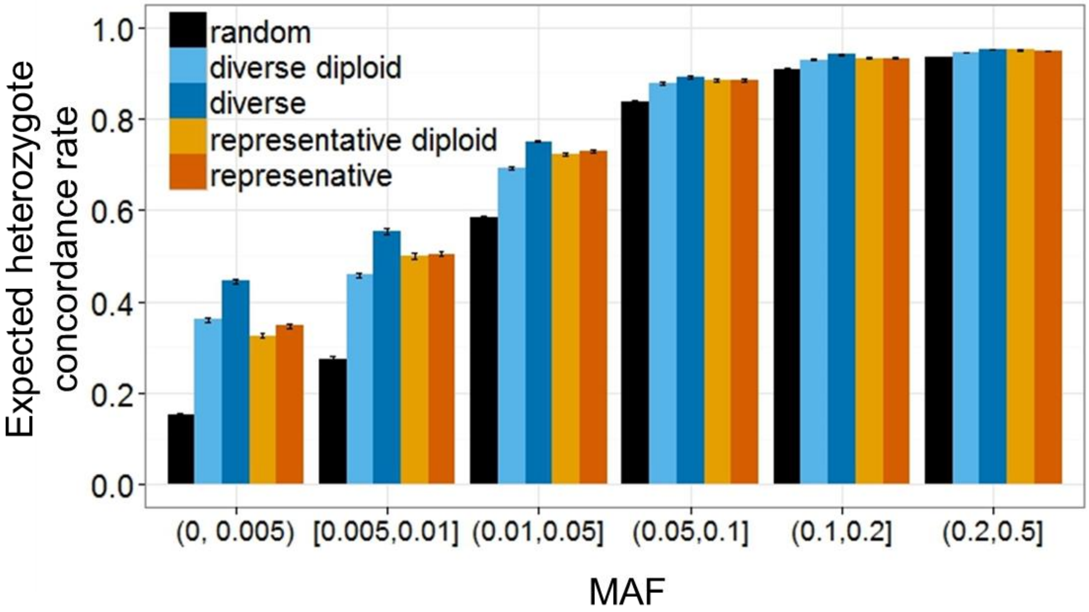

Chapter 5 Conclusion

The technological advancements allow investigators to use next-generation sequencing data to identify rare genetic variants for complex diseases. However, association tests of rare variants require a large sample size to obtain enough counts of the minor alleles to gain sufficient statistical power and it is still expensive to sequence a large sample. Genotype imputation can augment sequence data while challenges still remain, such as imputations of data with population or family structures and imputations of rare variants. In this dissertation I develop an approach to apply genotype imputation to family-based data and propose two sampling strategies based on existing array data for planning sequencing studies with limited budgets.

In Chapter 2, I propose a novel strategy for imputing family-based genotype data in an association study for bipolar disorder, with the aim to fine mapping risk loci that contribute to a previous observed linkage peak at 8q24. Using about 3,000 SNPs across the region in 3,512 individuals from 737 families with European ancestry including the families used in previous linkage analysis, I perform a detailed single-maker analysis under different genetic models. In addition, I impute the genotypes for all the HapMap markers in the assayed region. The results show marginal significance of loci near three genes.

The reasons for no statistically significant signals found might be multifold. First, bipolar disorder is a highly heterogeneous disease, both phenotypically and genetically. Second, the limitations of the software on complex family structures may also reduce power in the analysis. Third, there may be no risk loci in the studied region.

Future directions for this project involve further characterizing the disease features and identifying more variants in the region through sequencing. Because of the high heterogeneity of bipolar disorder, selecting a clinically more homogeneous subset of patients might increase the power to detect risk loci that contribute to a certain pathway. For example, one can select only patients diagnosed with bipolar I disorder, or bipolar patients who also have anxiety disorder (Saunders et al. 2009; Saunders et al. 2012). In addition, one can identify the estimated number of shared haplotypes at 8q24 in the sample and sequence individuals who carry those shared haplotypes. Once new rare variants are identified in this region, one can test associations of these novel rare variants with bipolar disorder using the entire study sample or other samples through cost-effective customized arrays.

In Chapter 3 and Chapter 4, I investigate on how to use genotype imputation when planning sequencing studies by proposing two sampling strategies based on genotypes from existing array data. The goal is to find an optimal subset to sequence, in a sense that one can identify the maximal number of variants via sequencing the selected subset, and obtaining the maximal imputation accuracy when using the sequenced subset as a reference panel to get the sequences of the entire study sample. In Chapter 3, I focus on the property of the selected panel only and aim to make the selected haplotypes to be most distinct from each other in order to incorporate the maximal diversity of the sample into the selected panel. To achieve this goal, I adapt the phylogenetic diversity and a greedy algorithm to select the subset with the maximal subtree length (Pardi and Goldman 2005; Steel 2005). The assumption is that the number of mutation events is proportional to the evolutional time and the subset with maximal tree length represents the longest evolutionary time. In Chapter 4, I consider both the selected haplotypes and the unselected haplotypes when identifying the optimal panel. I propose another sampling strategy for sequencing studies, termed as the most representative subset. The goal is to select a subset such that every unselected haplotype in the study sample has at least one similar haplotype in the selected subset that can be used as its template in imputation.

In summary, I present two sampling strategies for planning sequence studies. Both strategies provide better performance than randomly selected samples. Both methods allow for incorporating other selection criteria. For example, one can treat individuals selected from other criteria as an initial set and apply the algorithm to the initial set as an extension. Based on the results from the simulated data as well as the real sequence data from the 1000 Genomes Project, I recommend a few guidelines which strategy investigators can choose in order to identify maximal polymorphic sites from a study sample when planning sequencing studies with existing genotype data: 1) For study individuals that are from one population, the representative reference panel is more likely to provide a better performance. 2) For study individuals that are from closely related populations, the diverse reference panel is more likely to provide a better performance. 3)

The diverse panel might work better than the representative panel when imputing short regions (e.g., regions of a few hundred kbs), whereas the representative panel might work better when imputing longer regions, e.g., a few Mbs or longer. 4) The differences between reference panels become smaller when more individuals are sequenced.

Future work for the most diverse reference panel involves better characterizing the data on which the algorithm can work best. For example, Bordewich et al. (2008) found that selecting the most diverse subset may not always be the best choice in certain tree topologies and proposed an alternative strategy. However, they did not provide a systemic measure to categorize the tree topologies. One can better use the algorithm if there is a summary statistics that provides such information. Future work for the most representative panel involves algorithm optimization. The hill-climbing based approach is easy to implement and takes limited memory. But it is often not efficient in finding a solution and the solution may not be globally optimal. I intend to further optimize the algorithm by borrowing ideas from tag SNPs selection as its idea is similar as the most representative panel.

Future directions for both panels include 1) further characterizing the two sampling strategies in order to determine when they work the best. My goal is to provide guidelines for investigators to select a subset to sequence when they plan sequencing studies. Based on simulation results, I have provided several suggestions on which sampling strategy to use with a specific study sample. In general, the most diverse algorithm aims to maximize variants discovery while the representative algorithm aims to find the maximal imputation accuracy. I intend to characterize the study samples from population genetics perspective to see if there exists some summary statistics of a study sample that can be used to select the best panel for the specific study sample. 2) Quantifying the gain by using the proposed panels than a randomly selected panel, either economically and statistically. 3) Combining existing sequence data such as the data from the 1000 Genomes Project when selecting the optimal reference panel. For example, one can identify a subset of the study sample that shares common fragments with sequences from the 1000 Genomes Project and get the sequences the selected subset by imputation using data from the 1000 Genomes Project as references, while sequencing the rest of the study sample that are more different from the sequences from the 1000 Genomes Project. 4) Incorporating phenotype information. Ignoring phenotype information in selecting a subset to sequence may bias the downstream disease association tests. One can avoid the problem by considering sequencing as a SNP discovery step and get genotypes for the entire study sample or other samples through more cost-effective customized arrays for association tests. Answering these questions and better characterizing the two strategies will certainly provide investigators more information in choosing the optimal strategy to use when planning sequencing studies in the future.

In summary, in this dissertation, I have addressed challenges and have provided strategies in applying genotype imputation to data with family structures and to augment sequence data in next-generation sequencing studies. These strategies provide practical solutions to the problems arising from identifying risk variants, especially rare risk variants for complex diseases. I have presented results in applying one of my proposed methods to bipolar disorder, but all the proposed methods can be applied to other common complex disorders. Currently thoughts of GWAS have been performed with millions of individuals involved. I expect that investigators have started to sequence them and will eventually get the sequences for all these individuals with phenotypes of interest either by direct sequencing or high quality imputation. My dissertation work thus has the potential to provide investigators a cost-effective way in get the high quality sequences of a large study sample with limited budget.

Bibliography

Askland K, Read C, J M. 2009. Pathways-based analyses of whole-genome association study data in bipolar disorder reveal genes mediating ion channel activity and synaptic neurotransmission. *Hum Genet* **125(1)** (1): 63-79.

Avramopoulos D, Willour VL, Zandi PP, Huo Y, MacKinnon DF, Potash JB, DePaulo JR, Jr., McInnis MG. 2004. Linkage of bipolar affective disorder on chromosome 8q24: follow-up and parametric analysis. *Mol Psychiatry* **9**(2): 191-196.

Badner JA, Gershon ES. 2002. Meta-analysis of whole-genome linkage scans of bipolar disorder and schizophrenia. *Mol Psychiatry* **7**(4): 405-411.

Barnett JH, Smoller JW. 2009. The genetics of bipolar disorder. *Neuroscience* **164**(1): 331-343.

Bodmer W, Bonilla C. 2008. Common and rare variants in multifactorial susceptibility to common diseases. *Nat Genet* **40**(6): 695-701.

Bordewich M, Rodrigo AG, Semple C. 2008. Selecting taxa to save or sequence: desirable criteria and a greedy solution. *Syst Biol* **57**(6): 825-834.

Brown AHD. 1989. Core collections: a practical approach to genetic resources management. *Genome* **31**(2): 818-824.

Browning BL, Yu Z. 2009. Simultaneous genotype calling and haplotype phasing improves genotype accuracy and reduces false-positive associations for genome-wide association studies. *Am J Hum Genet* **85**(6): 847-861.

Bryant D. 2005. On the Uniqueness of the Selection Criterion in Neighbor-Joining. *J Classif* **22**(3-15).

Burmeister M, McInnis MG, Zöllner S. 2008. Psychiatric genetics: progress amid controversy. *Nat Rev Genet* **9**(7): 527-540.

Carter CJ. 2007. Multiple genes and factors associated with bipolar disorder converge on growth factor and stress activated kinase pathways controlling translation initiation: implications for oligodendrocyte viability. *Neurochem Int* **50**(3): 461-490.

Chumakov I, Cohen D, Macciardi F. 2006. Compositions and methods for treating mental disorders. US.

Cichon S, Schumacher J, Muller DJ, Hurter M, Windemuth C, Strauch K, Hemmer S, Schulze TG, Schmidt-Wolf G, Albus M et al. 2001. A genome screen for genes predisposing to bipolar affective disorder detects a new susceptibility locus on 8q. *Hum Mol Genet* **10**(25): 2933-2944.

Cirulli ET, Goldstein DB. 2010. Uncovering the roles of rare variants in common disease through whole-genome sequencing. *Nat Rev Genet* **11**(6): 415-425.

Cohen JC, Kiss RS, Pertsemlidis A, Marcel YL, McPherson R, Hobbs HH. 2004. Multiple rare alleles contribute to low plasma levels of HDL cholesterol. *Science* **305**(5685): 869-872.

De Mooij-van Malsen AJ, van Lith HA, Oppelaar H, Hendriks J, de Wit M, Kostrzewa E, Breen G, Collier DA, Olivier B, Kas MJ. 2009. Interspecies trait genetics reveals association of Adcy8 with mouse avoidance behavior and a human mood disorder. *Biol Psychiatry* **66**(12): 1123-1130.

Dick DM, Foroud T, Flury L, Bowman ES, Miller MJ, Rau NL, Moe PR, Samavedy N, El-Mallakh R, Manji H et al. 2003. Genomewide linkage analyses of bipolar disorder: a new sample of 250 pedigrees from the National Institute of Mental Health Genetics Initiative. *Am J Hum Genet* **73**(1): 107-114.

Endicott J, Spitzer RL. 1978. A diagnostic interview: the schedule for affective disorders and schizophrenia. *Arch Gen Psychiatry* **35**(7): 837-844.

Faith DP. 1992. Conservation evaluation and phylogenetic diversity. *Biol Conserv* **61**: 1-10.

Ferreira MA, O'Donovan MC, Meng YA, Jones IR, Ruderfer DM, Jones L, Fan J, Kirov G, Perlis RH, Green EK et al. 2008. Collaborative genome-wide association analysis supports a role for ANK3 and CACNA1C in bipolar disorder. *Nat Genet* **40**(9): 1056-1058.

Frazer KA Ballinger DG Cox DR Hinds DA Stuve LL Gibbs RA Belmont JW Boudreau A Hardenbol P Leal SM et al. 2007. A second generation human haplotype map of over 3.1 million SNPs. *Nature* **449**(7164): 851-861.

Fridley BL, Jenkins G, Deyo-Svendsen ME, Hebbring S, Freimuth R. 2010. Utilizing genotype imputation for the augmentation of sequence data. *PloS One* **5**(6): e11018.

Gargus JJ. 2006. Ion channel functional candidate genes in multigenic neuropsychiatric disease. *Biol Psychiatry* **60**(2): 177-185.

Gibson G. 2011. Rare and common variants: twenty arguments. *Nat Rev Genet* **13**(2): 135-145.

Gopalakrishnan S, Qin ZS. 2006. TagSNP selection based on pairwise LD criteria and power analysis in association studies. *Pac Symp Biocomput*: 511-522.

Hao K, Chudin E, McElwee J, Schadt EE. 2009. Accuracy of genome-wide imputation of untyped markers and impacts on statistical power for association studies. *BMC Genet* **10**: 27.

Howie B, Fuchsberger C, Stephens M, Marchini J, Abecasis GR. 2012. Fast and accurate genotype imputation in genome-wide association studies through pre-phasing. *Nat Genet* **44**(8): 955-959.

Howie BN, Donnelly P, Marchini J. 2009. A flexible and accurate genotype imputation method for the next generation of genome-wide association studies. *PLoS Genet* **5**(6): e1000529.

Huang L, Jakobsson M, Pemberton TJ, Ibrahim M, Nyambo T, Omar S, Pritchard JK, Tishkoff SA, Rosenberg NA. 2011. Haplotype variation and genotype imputation in African populations. *Genet Epidemiol* **35**(8): 766-780.

Huang L, Li Y, Singleton AB, Hardy JA, Abecasis G, Rosenberg NA, Scheet P. 2009. Genotype-imputation accuracy across worldwide human populations. *Am J Hum Genet* **84**(2): 235-250.

Hudson RR. 2002. Generating samples under a Wright-Fisher neutral model of genetic variation. *Bioinformatics* **18**(2): 337-338.

Jewett EM, Zawistowski M, Rosenberg NA, Zöllner S. 2012. A coalescent model for genotype imputation. *Genetics* **194**(4): 1239-1255.

Jostins L, Morley KI, Barrett JC. 2011. Imputation of low-frequency variants using the HapMap3 benefits from large, diverse reference sets. *Eur J Hum Genet* **19**(6): 662-666.

Kang CJ, Marjoram P. 2012. A sample selection strategy for next-generation sequencing. *Genet Epidemiol* **36**(7): 696-709.

Lee KW, Woon PS, Teo YY, Sim K. 2012. Genome wide association studies (GWAS) and copy number variation (CNV) studies of the major psychoses: what have we learnt? *Neurosci Biobehav Rev* **36**(1): 556-571.

Li Y, Sidore C, Kang HM, Boehnke M, Abecasis GR. 2011. Low-coverage sequencing: implications for design of complex trait association studies. *Genome Res* **21**(6): 940-951.

Li Y, Willer C, Sanna S, Abecasis G. 2009. Genotype imputation. *Annu Rev Genomics Hum Genet* **10**: 387-406.

Li Y, Willer CJ, Ding J, Scheet P, Abecasis GR. 2010. MaCH: using sequence and genotype data to estimate haplotypes and unobserved genotypes. *Genet Epidemiol* **34**(8): 816-834.

Macayran JF, Brodie SG, Rao PN, O'Connor MJ, Gray JA, Ciarimboli B, Dipple KM. 2006. Duplication 8q22.1-q24.1 associated with bipolar disorder and speech delay. *Bipolar Disord* **8**(3): 294-298.

Marchini J, Howie B. 2010. Genotype imputation for genome-wide association studies. *Nat Rev Genet* **11**(7): 499-511.

Marchini J, Howie B, Myers S, McVean G, Donnelly P. 2007. A new multipoint method for genome-wide association studies by imputation of genotypes. *Nat Genet* **39**(7): 906-913.

McInnis MG, Lan TH, Willour VL, McMahon FJ, Simpson SG, Addington AM, MacKinnon DF, Potash JB, Mahoney AT, Chellis J et al. 2003. Genome-wide scan of bipolar disorder in 65 pedigrees: supportive evidence for linkage at 8q24, 18q22, 4q32, 2p12, and 13q12. *Mol Psychiatry* **8**(3): 288-298.

McKhann HI, Camilleri C, Berard A, Bataillon T, David JL, Reboud X, Le Corre V, Caloustian C, Gut IG, Brunel D. 2004. Nested core collections maximizing genetic diversity in Arabidopsis thaliana. *Plant J* **38**(1): 193-202.

McQueen MB, Devlin B, Faraone SV, Nimgaonkar VL, Sklar P, Smoller JW, Abou Jamra R, Albus M, Bacanu SA, Baron M et al. 2005. Combined analysis from eleven linkage studies of bipolar disorder provides strong evidence of susceptibility loci on chromosomes 6q and 8q. *Am J Hum Genet* **77**(4): 582-595.

McQuillin A, Rizig M, Gurling HM. 2007. A microarray gene expression study of the molecular pharmacology of lithium carbonate on mouse brain mRNA to understand the neurobiology of mood stabilization and treatment of bipolar affective disorder. *Pharmacogenet Genomics* **17**(8): 605-617.

Merikangas KR, Akiskal HS, Angst J, Greenberg PE, Hirschfeld RM, Petukhova M, Kessler RC. 2007. Lifetime and 12-month prevalence of bipolar spectrum disorder in the National Comorbidity Survey replication. *Arch Gen Psychiatry* **64**(5): 543-552.

Nee S, May RM. 1997. Extinction and the loss of evolutionary history. *Science* **278**(5338): 692-694.

Nelson MR, Wegmann D, Ehm MG, Kessner D, St Jean P, Verzilli C, Shen J, Tang Z, Bacanu SA, Fraser D et al. 2012. An abundance of rare functional variants in 202 drug target genes sequenced in 14,002 people. *Science* **337**(6090): 100-104.

Nothnagel M, Ellinghaus D, Schreiber S, Krawczak M, Franke A. 2009. A comprehensive evaluation of SNP genotype imputation. *Hum Genet* **125**(2): 163-171.

Nurnberger JI, Jr., Blehar MC, Kaufmann CA, York-Cooler C, Simpson SG, Harkavy-Friedman J, Severe JB, Malaspina D, Reich T. 1994. Diagnostic interview for genetic studies. Rationale, unique features, and training. NIMH Genetics Initiative. *Arch Gen Psychiatry* **51**(11): 849-859; discussion 863-844.

Pardi F, Goldman N. 2005. Species choice for comparative genomics: being greedy works. *PLoS Genet* **1**(6): e71.

Pasaniuc B, Avinery R, Gur T, Skibola CF, Bracci PM, Halperin E. 2010. A generic coalescent-based framework for the selection of a reference panel for imputation. *Genet Epidemiol* **34**(8): 773-782.

Pei YF, Zhang L, Li J, Deng HW. 2010. Analyses and comparison of imputation-based association methods. *PloS One* **5**(5): e10827.

Perez J, Tardito D, Mori S, Racagni G, Smeraldi E, Zanardi R. 2000. Abnormalities of cAMP signaling in affective disorders: implication for pathophysiology and treatment. *Bipolar Disord* **2**(1): 27-36.

Reeves PA, Panella LW, Richards CM. 2012. Retention of agronomically important variation in germplasm core collections: implications for allele mining. *Theor Appl Genet* **124**(6): 1155-1171.

Russell S, Norviq P. 2009. Beyond classical search. In *Artificial Intelligence: A Modern Approach,* pp. 120-129. Prentice Hall.

Saitou N, Nei M. 1987. The neighbor-joining method: a new method for reconstructing phylogenetic trees. *Mol Biol Evol* **4**(4): 406-425.

Saunders EF, Fitzgerald KD, Zhang P, McInnis MG. 2012. Clinical features of bipolar disorder comorbid with anxiety disorders differ between men and women. *Depress Anxiety* **29**(8): 739-746.

Saunders EF, Zhang P, Copeland JN, McLnnis MG, Zollner S. 2009. Suggestive linkage at 9p22 in bipolar disorder weighted by alcohol abuse. *Am J Med Genet B, Neuropsychiatr Genet* **150B**(8): 1133-1138.

Schroeder BC, Kubisch C, Stein V, Jentsch TJ. 1998. Moderate loss of function of cyclic-AMP-modulated KCNQ2/KCNQ3 K+ channels causes epilepsy. *Nature* **396**(6712): 687-690.

Scott LJ, Muglia P, Kong XQ, Guan W, Flickinger M, Upmanyu R, Tozzi F, Li JZ, Burmeister M, Absher D et al. 2009. Genome-wide association and meta-analysis of bipolar disorder in individuals of European ancestry. *Proc Natl Acad Sci U S A* **106**(18): 7501-7506.

Selman B, Gomes CP. 2006. Hill-climbing Search. *Encyclopedia of Cognitive Science*.

Serretti A, Mandelli L. 2008. The genetics of bipolar disorder: genome 'hot regions,' genes, new potential candidates and future directions. *Mol Psychiatry* **13**(8): 742-771.

Shendure J, Ji H. 2008. Next-generation DNA sequencing. *Nat Biotechnol* **26**(10): 1135-1145.

Smoller JW, Finn CT. 2003. Family, twin, and adoption studies of bipolar disorder. *Am J Med Genet C Semin Med Genet* **123C**(1): 48-58.

Sokal R, Michener C. 1958. A statistical method for evaluating systematic relationships. *Univ Kans Sci Bull* **38**: 1409-1438.

Steel M. 2005. Phylogenetic diversity and the greedy algorithm. *Syst Biol* **54**(4): 527-529.

Stewart RJ, Chen B, Dowlatshahi D, MacQueen GM, Young LT. 2001. Abnormalities in the cAMP signaling pathway in post-mortem brain tissue from the Stanley Neuropathology Consortium. *Brain Res Bull* **55**(5): 625-629.

The 1000 Genomes Project Consortium. 2010. A map of human genome variation from population-scale sequencing. *Nature* **467**(7319): 1061-1073.

The International HapMap Consortium. 2005. A haplotype map of the human genome. *Nature* **437**(7063): 1299-1320.

Van Os J, Rutten BP, Poulton R. 2008. Gene-environment interactions in schizophrenia: review of epidemiological findings and future directions. *Schizophrenia bulletin* **34**(6): 1066-1082.

Wang JR, de Villena FP, Lawson HA, Cheverud JM, Churchill GA, McMillan L. 2012. Imputation of single-nucleotide polymorphisms in inbred mice using local phylogeny. *Genetics* **190**(2): 449-458.

Wigginton JE, Abecasis GR. 2005. PEDSTATS: descriptive statistics, graphics and quality assessment for gene mapping data. *Bioinformatics* **21**(16): 3445-3447.

Xia J, Wang Q, Jia P, Wang B, Pao W, Zhao Z. 2012. NGS catalog: A database of next generation sequencing studies in humans. *Hum Mutat* **33**(6): E2341-2355.

Zandi PP, Avramopoulos D, Willour VL, Huo Y, Miao K, Mackinnon DF, McInnis MG, Potash JB, Depaulo JR. 2007. SNP fine mapping of chromosome 8q24 in bipolar disorder. *Am J Med Genet B, Neuropsychiatr Genet* **144B**(5): 625-630.

Zandi PP, Zöllner S, Avramopoulos D, Willour VL, Chen Y, Qin ZS, Burmeister M, Miao K, Gopalakrishnan S, McEachin R et al. 2008. Family-based SNP association study on 8q24 in bipolar disorder. *Am J Med Genet B, Neuropsychiatr Genet* **147B**(5): 612-618.

Zawistowski M, Gopalakrishnan S, Ding J, Li Y, Grimm S, Zöllner S. 2010. Extending rare-variant testing strategies: analysis of noncoding sequence and imputed genotypes. *Am J Hum Genet* **87**(5): 604-617.

Zeggini E, Scott LJ, Saxena R, Voight BF, Marchini JL, Hu T, de Bakker PI, Abecasis GR, Almgren P, Andersen G et al. 2008. Meta-analysis of genome-wide association data and large-scale replication identifies additional susceptibility loci for type 2 diabetes. *Nat Genet* **40**(5): 638-645.

Zhang P, Xiang N, Chen Y, Sliwerska E, McInnis MG, Burmeister M, Zöllner S. 2010. Family-based association analysis to finemap bipolar linkage peak on chromosome 8q24 using 2,500 genotyped SNPs and 15,000 imputed SNPs. *Bipolar Disord* **12**(8): 786-792.